

Folding Behavior of Chaperonin-Mediated Substrate Protein

Wei-Xin Xu,¹ Jun Wang,¹ and Wei Wang^{1,2*}

¹National Laboratory of Solid State Microstructure and Department of Physics, Nanjing University, Nanjing, China

²Interdisciplinary Center of Theoretical Studies, Chinese Academy of Sciences, Beijing, China

ABSTRACT Chaperonin-mediated protein folding is complex. There have been diverse results on folding behavior, and the chaperonin molecules have been investigated as enhancing or retarding the folding rate. To understand the diversity of chaperonin-mediated protein folding, we report a study based on simulations using a simplified G \ddot{o} -type model. By considering effects of affinity between the substrate protein and the chaperonin wall and spatial confinement of the chaperonin cavity, we study the thermodynamics and kinetics of folding of an unfrustrated substrate protein encapsulated in a chaperonin cavity. The affinity makes the hydrophobic residues of the protein bind to the chaperonin wall, and a strong (or weak) affinity results in a large (or small) effect of binding. Compared with the folding in bulk, the folding in chaperonin cavity with different strengths of affinity shows two kinds of behaviors: one with less dependence on the affinity but more reliance on the spatial confinement effect and the other relying strongly on the affinity. It is found that the enhancement or retardation of the folding rate depends on the competition between the spatial confinement and the affinity due to the chaperonin cavity, and a strong affinity produces a slow folding while a weak affinity induces a fast folding. The crossover between two kinds of folding behaviors happens in the case that the favorable effect of confinement is balanced by the unfavorable effect of the affinity, and a critical affinity strength is roughly defined. By analyzing the contacts formed between the residues of the protein and the chaperonin wall and between the residues of the protein themselves, the role of the affinity in the folding processes is studied. The binding of the residues with the chaperonin wall reduces the formation of both native contacts and nonnative contact or mis-contacts, providing a loose structure for further folding after allosteric change of the chaperonin cavity. In addition, 15 single-site-mutated mutants are simulated in order to test the validity of our model and to investigate the importance of affinity. Inspiringly, our results of the folding rates have a good correlation with those obtained from experiments. The folding rates are inversely correlated with the strength of the binding interactions, i.e., the weaker the binding, the faster the folding. We also find that the inner hydro-

phobic residues have larger effects on the folding kinetics than those of the exterior hydrophobic residues. We suggest that, besides the confinement effect, the affinity acts as another important factor to affect the folding of the substrate proteins in chaperonin systems, providing an understanding of the folding mechanism of the molecular chaperonin systems. *Proteins* 2005;61:777–794.

© 2005 Wiley-Liss, Inc.

Key words: chaperonin cavity; substrate protein folding; G \ddot{o} -type model

INTRODUCTION

Protein folding is an important problem in molecular biology. The funnel-like landscape theory provides a paradigm for folding processes, which describes protein molecules “diffuse” towards their native structures on a rough landscape with a large funnel-like bias of energy.^{1–7} Many works of protein folding actually study the folding processes of protein molecules in vitro. However, it is very important to understand the folding processes of the protein molecules in vivo since nascent peptide chains must fold into their functional shapes, namely the native structures, and then these newly synthesized proteins play related functions in cells relying on their structures. The folding of proteins in vivo involves many factors, such as the competition between folding and aggregation of molecules in a crowded environment and the effects of other molecular machineries.^{8–12} The interactions between the protein molecules themselves and between other kinds of molecules introduce positive or negative effects for folding, resulting in more complex folding behaviors than those in vitro. These have been attracting wide interest.^{13–18}

A kind of molecular machinery associated with protein folding in vivo is the molecular chaperones, such as the heat shock proteins (HSP60, HSP70, and so on), which are

Grant sponsor: National Natural Science Foundation of China; Grant numbers: 90103031, 90403120, 10021001, 10204013, 10474041; Grant sponsor: Nonlinear Project of the NSM; Grant number: 973; Grant sponsor: FANEDD.

*Correspondence to: Prof. Wei Wang, Physics Department, Nanjing University, Nanjing 210093, China. E-mail: wangwei@nju.edu.cn

Received 21 December 2004; Revised 18 May 2005; Accepted 21 June 2005

Published online 17 October 2005 in Wiley InterScience (www.interscience.wiley.com). DOI: 10.1002/prot.20689

assemblages of some proteins themselves. The most common example of molecular chaperones is the GroEL/GroES chaperonin system in *Escherichia coli* (*E. coli*). This system consists of megadalton rings that mediate the essential ATP-dependent assistance of protein folding to the native state in a variety of cellular compartments, including the mitochondrial matrix, the eukaryotic cytosol, and the bacterial cytoplasm.¹⁹ How does the chaperonin system help the folding? This is still not very clear though there has been progress in understanding the chaperonin-mediated protein folding due to a number of experimental and theoretical studies. As a common view, the chaperonin system isolates the substrate proteins from a crowded environment or/and carries out a catalytic unfolding of the misfolded states of the substrate proteins or/and chooses the pathways to block some competing local minima.²⁰ From the perspective of the so-called Anfinsen cage,^{21–23} it is argued that the encapsulation of chaperones provides a space for a protein to perform its folding from the crowded cellular environment. Thus, the aggregation of substrate proteins is suppressed.^{10,12,24} In addition, a thermodynamic coupling mechanism for chaperonin-mediated unfolding to prevent the aggregation of substrate proteins has been proposed.²⁵ In addition to preventing aggregation during substrate protein folding, it has also been suggested that the spatial confinement in chaperonins makes the energy landscape of folding become smooth for some large proteins, either by preventing the formation of certain kinetically trapped intermediates or by facilitating their folding towards the compact native state.^{13,26} Remarkably, in accord with the predictions first made by Betancourt and Thirumalai that confinement smoothes the energy landscape,¹³ the SR1 experiment by Brinker and coworkers indicated that confinement alone can help proteins fold.²⁷ In addition, by analyzing the folding progresses of substrate proteins with the help of chaperonin, iterative annealing mechanism (IAM)²⁸ was proposed to interpret the functions of the chaperonin. Under the kinetic partition mechanism,^{29,30} the catalytic unfolding by binding with the chaperonin greatly helps the bad-folders or mis-folders to fold with many competitive intermediates.

Recently, several interesting experimental studies and theoretical modelings on the folding of proteins in systems with confined space showed some insights into the microscopic mechanisms of the chaperonin-assisted folding. The experiment of encapsulated proteins in silica matrix by Valentine et al. showed that the melting temperature of the α -lactalbumin is increased by as much as 32°C.³¹ The melting temperature of the single domain protein yeast frataxin is increased by almost 5°C.³² These experiments indicate that confinement can enhance the thermodynamic stability of proteins. It was also pointed out theoretically that the spatial confinement enhances the stability of the substrate protein.^{13,33–35} Additionally, this kind of geometrical effect can apparently increase the folding rate,^{23,33,35} and thus is considered one of the important functions of the chaperonin molecules. This information

really improves our understanding of the folding behaviors of the chaperone-assisted proteins.

The spatially geometrical restriction emphasizes the confinement on the conformational entropy of the protein chain. That is, by compressing the phase space of denatured states, the chaperonin decreases the space for searching the native basin of energy landscape. This is responsible for the acceleration of the folding as found in several previous studies. However, some experiments showed that the GroEL-mediated protein folding behaves differently. In the case of kinetics, for the stringent substrate protein RuBisCO, an obvious enhancement of the folding rate by adding GroEL molecules has been observed.²⁸ Nevertheless, the folding of protein CI2 or barnase by adding GroEL molecules is retarded.^{36,37} In the case of thermodynamics, the stability of proteins in a confined space is enhanced.^{31,32} However, Zahn et al. observed that the stability decreased in the presence of chaperonin molecules.¹⁵ Thus, an unfolding activity by the chaperonin systems was proposed based on the decrease of the thermodynamic stability which is reflected by a reversible lowering of the melting temperature in the presence of chaperonin molecules.¹⁵

As a matter of fact, these experimental observations cannot be simply explained using the argument based only on the geometrical restriction. Some experiments also illustrated the importance of the binding between the substrate proteins and the chaperonin wall. The crystal structure of the GroEL/GroES/ADP complex shows some changes in the size and the internal surface of the GroEL cavity after the allosteric transition induced by ATP. It has been argued that this kind of change is related to the folding of the substrate proteins in the chaperonin cavity.^{29,38} These imply that the interactions between the substrate proteins and the GroEL cavity should take an obligatory role in modeling the GroEL-mediated folding. Therefore, in order to understand the diverse experimental results, interactions and some other factors should be considered when building a better model rather than considering only a geometrical view for the GroEL chaperonin system.

Actually, some works related to the folding of protein molecules in chaperonin systems have been done using theoretical methods^{39,40} and numerical simulations with lattice models.^{13,14} The change of free energy landscape and related effects has been widely discussed, and the effect of confinement and interactions were of initial concern. However, the related folding of proteins in chaperonin systems is quite complicated and still attracts many researchers.^{18,33–35,41,42} In a work by Jewett et al.,¹⁸ the folding of a highly frustrated protein within the hydrophobic chaperonin cavity was shown to be accelerated if the hydrophobicity of the chaperonin environment is moderate. However, the confinement effect of the chaperonin cavity was not specially discussed in their work. The confinement effect of the chaperonin cavity on the folding of unfrustrated proteins was reported by Takagi et al.³⁵ It was found that the confinement of the chaperonin cage can significantly accelerate the folding of a substrate

protein. But, the affinity between the substrate protein and the chaperonin wall was ignored in their work.

In this report, we report an investigation on the effects of the interactions between substrate proteins and chaperonin molecules and of confinement on the folding processes of unfrustrated proteins in chaperonin cages. We focus our attention on the nonspecific hydrophobic interactions between the chaperonin wall and the residues of the substrate protein. In our model, some nonnative hydrophobic attractions with a van der Waals (VDW) formed between the residues and also between the residue and the GroEL wall are included. This kind of interactions mimics the environment for the substrate proteins in the GroEL cavity. By considering the attraction with the GroEL inner wall, the folding behaviors of the model proteins show a change from being promoted to being prohibited. With such an understanding, the difference of the interaction strengths in various chaperone systems could be a source to produce diverse behaviors of folding. This provides a general physical picture for the folding of the GroEL-protein complex beyond the model of a simple geometrical cavity. Concentrating on cases with large affinity between the proteins and the GroEL wall (similar to the first step of the GroEL-mediated protein folding processes), we find that the GroEL acts as a helper to destruct the compact mis-folded states of the proteins. The binding with the wall may also provide a way to prevent the proteins from mis-folding, which enables the proteins in the chaperonin cavity to fold into their native structures. In addition, the effects of mutations for a series of hydrophobic residues of a substrate protein are studied. The simulation results show a good agreement with experiments, and further support the importance of interaction between the substrate protein and the chaperone wall. The combination of the effects of confinement and affinity results in a two-step scheme of folding of the substrate protein in chaperones, which resembles partially the microscopic picture of the iterative annealing mechanism (IAM).

MODEL AND METHODS

G \bar{o} -Type Model of the Substrate Protein

In this work, the G \bar{o} -type interactions are employed to construct the model of the substrate protein. It includes the interactions related to the virtual bonds, angles, dihedral angles, and nonbonded pairs of the C $_{\alpha}$ atoms.^{43–50} This kind of G \bar{o} -type interaction has been successfully applied in modeling the folding processes in vitro.^{44–46,51–54} The parameters for the G \bar{o} -type interaction are similar to those used by Clementi et al.⁴⁴ As a simple model, the native contact pairs of residues are assigned as an attractive interaction of a 12–10 Lennard-Jones (LJ) potential. Here, two residues are defined as a “native contact” if the distance between any pair of nonhydrogen atoms belonging to these two residues, respectively, is shorter than 5Å in the native conformation. In most previous works with the G \bar{o} -type models, the nonnative interactions are neglected. However, recent studies showed that the nonnative interactions have a significant effect on both folding and stability.^{55–58} Here, we take into account

the nonnative interactions as follows. First, all the residues can be divided into two kinds of residues, namely the hydrophobic (H-type) and the polar (P-type). Here, the H-type and the P-type residues are classified as (C, W, F, V, I, L, M, Y) and (A, R, D, E, K, P, S, T, N, H, G, Q), respectively, according to the results by Wang and Wang.⁵⁹ Then, there are three kinds of interactions, i.e., the HH-type, the HP-type, and the PP-type. Since the HH-type interactions are argued to be the main driving force for folding,⁶⁰ they are considered as a 12-6 (LJ) potential with the distance of the regular hard-core contact, i.e., 4Å, as the equilibrium distance. Differently, the interactions of the HP-type and the PP-type residue pairs are considered as repulsive potentials with a hard core. Of course, the interaction is not taken into account if two residues are already assigned as a native contact. These nonnative interactions may alter the structures of the denatured state ensemble and partially mimic the effective interactions created by solvents, producing a more realistic folding process. It is also tested that these nonnative interactions do not alter the native state of the model protein due to the rigidity of the native state.

Thus, the potential V of the protein is given as

$$\begin{aligned}
 V &= V_{\text{bonded}} + V_{\text{bond-angle}} + V_{\text{dihedral}} + V_{\text{non-bonded}} \\
 &= \sum_{\text{bonds}}^{N-1} K_r (r - r_0)^2 + \sum_{\text{bond-angles}}^{N-2} K_{\theta} (\theta - \theta_0) \\
 &\quad + \sum_{\text{dihedrals}}^{N-3} \{K_{\phi}^{(1)} [1 - \cos(\phi - \phi_0)] \\
 &\quad + K_{\phi}^{(3)} [1 - \cos 3(\phi - \phi_0)]\} \\
 &\quad + \sum_{i < j - 3}^{\text{native}} \epsilon(i, j) \left[5 \left(\frac{\sigma_{ij}}{r_{ij}} \right)^{12} - 6 \left(\frac{\sigma_{ij}}{r_{ij}} \right)^{10} \right] \\
 &\quad + \sum_{i < j - 3, hh}^{\text{non-native}} \bar{\epsilon}(i, j) \left[\left(\frac{\sigma_0}{r_{ij}} \right)^{12} - 2 \left(\frac{\sigma_0}{r_{ij}} \right)^6 \right] \\
 &\quad + \sum_{i < j - 3, else}^{\text{non-native}} \epsilon \left(\frac{\sigma_0}{r_{ij}} \right)^{12}. \tag{1}
 \end{aligned}$$

Here, r , θ , and ϕ represent the virtual bond length, bond-angle, and dihedral angle, respectively; r_{ij} is the spatial distance between the i -th and the j -th residues and σ_{ij} is their distance in the native conformation. r_0 , θ_0 , and ϕ_0 correspond to the values extracted from the native coordinates of the substrate protein. N denotes the chain length. All other parameters are set as follows: $\sigma_0 = 4\text{Å}$, $K_r = 100\epsilon$, $K_{\theta} = 20\epsilon$, $K_{\phi}^{(1)} = \epsilon$, $K_{\phi}^{(3)} = 0.5\epsilon$. Especially, in order to consider the information encoded in the protein chain, the number of pairs of nonhydrogen atoms for a contact is taken into account as a weight $\epsilon(i, j)$ in native contact interactions. Here, $\epsilon(i, j)$ is defined as $(N_c N_{ij} / \sum_{(i, j)} n_{ij}) \epsilon$ where N_c is the total native contact num-

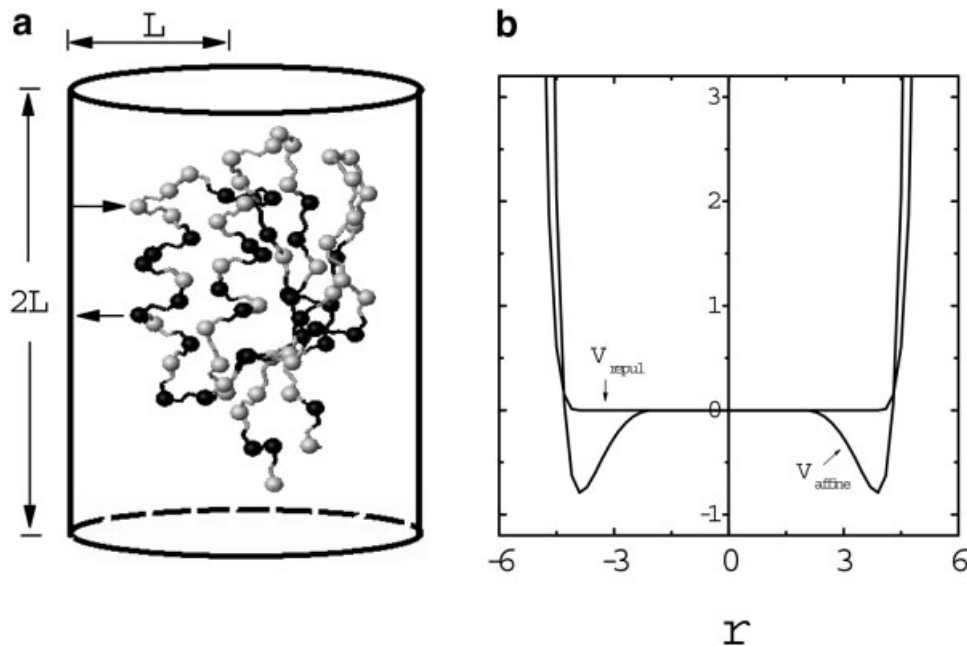


Fig. 1. The sketch map for the substrate protein Ada2h encapsulated in the chaperonin cavity (a). The hydrophobic residues are shown as black balls and the hydrophilic residues as gray balls. The arrows represent the attractive and repulsive interactions. The repulsive interaction V_{repul} between the hydrophilic residues and the wall and the affine interaction V_{affine} between the hydrophobic residues and the chaperonin wall are plotted, respectively (b).

bers, N_{ij} is the total number of atom-pairs between two native contacting residues, n_{ij} is the number of atom-pairs between residues i and j . $\bar{\epsilon}(i,j)$ is the average value of $\epsilon(i,j)$. For a certain conformation, a contact between two residues i and j is formed if the distance between their C_{α} atoms is shorter than γ times the native distance σ_{ij} . It has been shown that the results are not strongly dependent on the choice made for the cut-off distance γ .⁶¹ In this work we used $\gamma = 1.2$. We then use a reaction coordinate, $Q(t)$, to measure the nativeness of the conformation of the protein at time t . Here $Q(t)$ is defined as the ratio of the number of formed native contacts to that at the native structure. The native ensemble is assumed at $Q \geq 0.9$.

An α/β sandwich fold is found to be a common structural motif as the GroEL substrate proteins.²⁶ Thus, we choose the Human Procarboxypeptidase A2 (Ada2h, PDB code: 1aye) and Chymotrypsin Inhibitor-2 (CI2, PDB code: 1coa) as two examples of the substrate proteins. Furthermore, both proteins are two-state, single-domain proteins, which consist of 78 residues and 64 residues, respectively. Simulations for these two small proteins are maneuverable. Especially, the folding of protein CI2 in chaperonin GroEL has been experimentally studied by Itzhaki et al.³⁷ This offers a good chance to compare our simulations with experiments to understand the mechanism of GroEL-associated folding processes. The experimental results also help us check the validity of the simplified models.

Chaperonin Model

The cylindrical structure of the GroEL/GroES complex has already been experimentally determined.^{62–64} The

crystal structure of the GroEL shows that it is a double-ring oligomer consisting of back-to-back seven-member rings. It has an overall cylindrical structure divided into two nonconnected cavities in which the substrate proteins can be sequestered. The co-chaperonin GroES is composed of seven subunits and serves as a dome on the cylindrical structure.⁶⁵ In this work, the chaperonin system is modeled as a cylindrical cavity with a characteristic length L (the radius), which is scaled in a unit of 3.8\AA , and the diameter and height are equal as shown in Figure 1. The folding of the substrate protein in the *E. coli* GroEL/ES chaperonin system is modeled as follows. The substrate protein molecule is confined in the cylindrical GroEL cavity for performing its folding. The cavity introduces two effects, i.e., one is the spatial confinement and the other is the affinity for the residues of the substrate protein. The spatial confinement makes the protein move only in a small space and the affinity makes the residues interact, either attract or repulse, with the cavity wall. In the case of GroEL, the substrate protein interacts with the wall of the cavity nonspecifically. Only hydrophobicity contributes essentially. The experiments and theoretical models all suggested that the GroEL chaperonin affects the nonnative states of the substrate proteins more than their native states.

Under such considerations, the effects of confinement and nonspecific interactions will dominate the folding of the substrate protein. This is due to the fact that once the substrate protein is sequestered in the chaperonin cavity, other effects such as pH, ionic strength, and composition of various molecules, redox potential, among others, would

be excluded except the confinement effect. In addition, the affinity between the protein and the cavity wall is also important since the interior of the GroEL cavity upon complexation with the substrate and GroES is, in fact, moderately hydrophobic.¹³ Moreover, the chaperonin can assist folding of various proteins in a nonspecific manner, and thus any specific interactions between the substrate protein and the inner wall due to the intrinsic features of protein itself may not be crucial especially when the Gō-type interactions are used. Therefore, confinement, which restricts the conformational space of the protein chain, and interactions between the protein and the inner wall of cavity, are primary factors for the folding of substrate proteins in chaperonin system. Additionally, to investigate the complicated behaviors of chaperone-mediated protein folding, both the substrate protein and chaperone should be modeled in a sufficiently simple manner. Thus, a simplified model mainly focusing on effects of confinement and affinity is applicable. Previously, lattice protein models were used by Chan and Dill¹⁴ and Betancourt and Thirumalai.¹³ In contrast, in our work an off-lattice model is used.

Though the structure of the GroEL system is clear, the dynamic processes and the underlying mechanism of GroEL-associated folding is not well understood. Based on experimental results^{66–68} and theoretical arguments,^{13,28} a phenomenological working cycle for the GroEL/GroES chaperonin system was proposed. There are four steps in the working cycle¹³: (1) The substrate protein is encapsulated in the GroEL cavity; (2) ATP and GroES take effect, which doubles the volume of the GroEL cavity; (3) The hydrolysis of ATP in the cis-ring takes place in a quantified fashion; and (4) ATP is bound to the trans-ring, which primes the release of GroES and the substrate protein from the cis side. The substrate protein was argued to fold into its native state within several working cycles with the help of the GroEL/GroES chaperonin system. However, it was also found that a single binding event would be sufficient to accelerate the folding,⁶⁹ which implies that the binding event is trifling, but may be important for folding processes. Some other experiments further suggest such an idea. The rhodanese (another stringent GroEL/ES substrate protein) does not unbind from the GroEL during each cycle of the ATP binding and hydrolysis.^{8,70,71} In addition, it was shown that when the release of the GroES is blocked by the nonhydrolyzable ATP analog or a designed single-ring mutant SR1, folding of the sequestered rhodanese goes to completion.⁷² This indicates that for some substrate proteins it is possible to reach the native conformation while still binding with the GroEL and the binding could be helpful for folding in GroEL.

In the present work, we consider a single binding event and study the folding of substrate protein confined within the chaperonin cavity. This step corresponds to the binding of the substrate protein to the hydrophobic apical domain of the GroEL molecule (steps 1 and 2 in the working cycle). In such a case, the chaperonin wall is hydrophobic. Thus, the interactions between the residues of the substrate protein and the chaperonin wall are considered as hydrophobic interactions, which reflect the

hydrophobic nature of the binding between the chaperonin GroEL and the substrate protein.⁷³ Here, only the affinity of the hydrophobic residues between the chaperonin wall is introduced. This is similar to the consideration related to the intra-chain interactions. As shown in Figure1, a 4-2 LJ potential V_{affine} for such interactions is introduced. The equilibrium is reached when the distance between the residues and wall is 2Å , consistent with the hard-core radius of residue σ_0 defined above. The interactions between the hydrophilic residues and the chaperonin wall takes a repulsive potential V_{repul} only, which is the same as that used by Takagi et al.³⁵ In details, the interactions between the chaperonin wall and the hydrophobic (or the hydrophilic) residues V_{affine} (or V_{repul}) have the forms

$$V_{affine} = [V'(r_i) - V'(r_c)]$$

$$- \frac{dV'(r_i)}{dr_i} \Big|_{r_i=r_c} (r_i - r_c) \Theta(r_c - r_i), \quad (2)$$

$$V_{repul} = \sum_i 50 \in \left[\left(\frac{\sigma_0}{2r_i} \right)^4 - 2 \left(\frac{\sigma_0}{2r_i} \right)^2 + 1 \right] \Theta \left(\frac{\sigma_0}{2} - r_i \right), \quad (3)$$

$$V' = \sum_i h \in \left[\left(\frac{\sigma_0}{2r_i} \right)^4 - 10 \left(\frac{\sigma_0}{2r_i} \right)^2 \right]. \quad (4)$$

The potentials V_{affine} and V_{repul} are all shifted according to their cutoff distances. In Eq.(2), r_i is the distance between the i -th residue and the chaperonin wall; h represents the strength of the affinity, i.e., the strength of interactions between the hydrophobic residues and the wall; r_c is the cutoff distance of the affine potential set as $2\sigma_0$.

Langevin Dynamics

In this work, the folding is performed by using the Langevin dynamics

$$m\dot{v}(t) = F(t) - \gamma v(t) + \Gamma(t), \quad (5)$$

where v , \dot{v} and m represent the velocity, acceleration, and the mass of a bead, respectively; $F = -\nabla V_{total}$ is the force of potential; γ is the viscosity constant and $\gamma = 0.05\tau^{-1}$ is set. Here $V_{total} = V + V_{affine}$ is for the H-type residues (or $V_{total} = V + V_{repul}$ for the P-type residues). τ is the time unit. At low values of friction, τ is consistent with the period of oscillations and its minimum value is equal to $(ma^2/\epsilon)^{1/2}$ where a is the van der Waals radius of the residues and is taken as 5Å , m is of the order of 3×10^{-22} g, and ϵ is the strength of contact and is of the order of 1 kcal/mol. Thus, τ is equal to about 3ps. Γ is the random force that satisfies the Einstein relationship $(\Gamma(t)\Gamma(t')) = 6\gamma k_B T \delta(t - t')$ where k_B is the Boltzmann constant, T is absolute temperature, t is time, and $\delta(t - t')$ is the Dirac delta function. The integration step is $\Delta t = 0.005\tau$. Initial unfolded states of the protein are obtained from an ensemble equilibrated at $2.4T_f^0$. Here T_f^0 is the folding temperature in bulk. Solving of the Langevin dynamics is realized by a leapfrog algorithm.

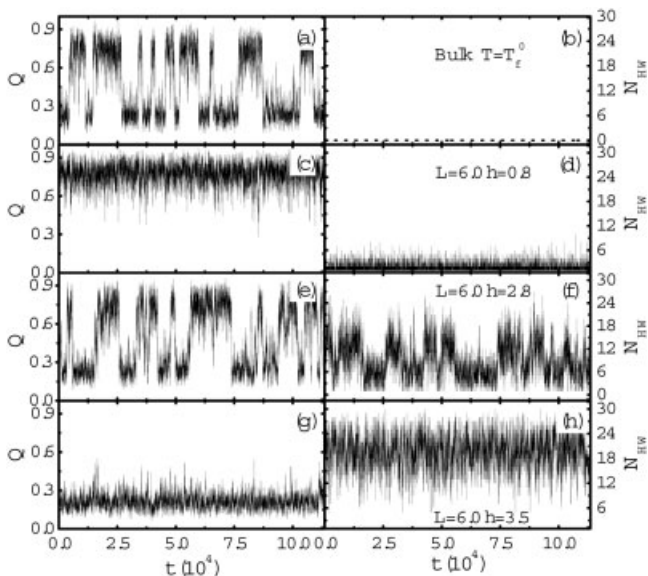


Fig. 2. The time evolution of $Q(t)$, the ratio of the number of the native contacts to that of the native conformation of the substrate protein, and the corresponding contact N_{HW} formed between the substrate protein and the chaperonin wall at the folding transition temperature in bulk T_f^0 and the radius $L = 6$. The folding in bulk (a,b), and in cavity with the affinity strength $h = 0.8$ (c,d), $h = 2.8$ (e,f), and $h = 3.5$ (g,h).

Thermodynamic Variable

Two-state cooperativity is an important feature of small proteins and is intensively investigated.^{74,75} Such a cooperativity is well characterized by Kaya and Chan⁷⁵ as

$$\kappa = 2T_{\max} \sqrt{k_B C_v T_{\max} / \Delta E_{tot}}, \quad (6)$$

where C_v is the heat capacity, T_{\max} is the peak temperature of C_v and ΔE_{tot} is the total change of energy between the folded state and unfolded state.

RESULTS AND DISCUSSION

Kinetics of Folding

Kinetics of spontaneous folding in chaperonin cavity are of experimental^{27,28,37,76} and theoretical interest.^{13,14,35} Many features have been illustrated in minimalist models previously.^{13,14,18,35} Here we present a detailed investigation on the kinetics of the substrate proteins encapsulated in the chaperonin cavity. Some kinetic results obtained are in accord with the findings by experiments^{28,77} and simulations,^{13,14} which validate the setup of our model. Moreover, some interesting phenomena are observed. A series of cases with various cavity sizes characterized by radius L and wall interactions depicted by affinity strength h were studied. The bulk case, namely the folding in the absence of the cavity, is used as reference for comparison. The results of the folding kinetics of protein in the chaperonin cavity are presented as follows.

The typical time evolutions of the native similarity $Q(t)$ to the native state of the substrate protein and contact number N_{HW} formed between the protein and the chaperonin wall are plotted in Figure 2. These results are obtained at temperature T_f^0 . In bulk case, the protein exhibits sharp

two-state transitions between the native state with high Q values and the denatured states with low Q values [see Fig. 2(a)]. When the substrate protein is encapsulated in the chaperonin cavity, the folding behaviors are altered as shown in Figure 2(c–h). For the chaperonin cavity with radius $L = 6.0$ and affinity $h = 0.8$, the substrate protein folds to its native state after a short time and stays there stably [see Fig. 2(c)]. The number of contacts N_{HW} is small, i.e., only about 4 contacts formed between the protein and the wall [Fig. 2(d)]. This means that when the affinity-induced interactions are not strong enough, the effect of spatial confinement dominates and enhances the folding. Interestingly, in the case of $L = 6.0$ and $h = 2.8$, the substrate protein again exhibits a sharp two-state folding [Fig. 2(e)]. The values of Q and N_{HW} hop up and down between the folded state and the unfolded states synchronously with a reverse phase [Fig. 2(e,f)]. That is, the native protein has few contacts with the wall, while in the nonnative states the protein contacts with wall largely. In this case, the affinity-induced binding of the substrate protein with the chaperonin wall is strong, which compromises the confinement effect. Thus, the folding behavior of the substrate protein is similar to that under bulk condition. Nevertheless, in the case of very strong affinity with $h = 3.5$, the protein is tightly bound to the wall with high values of $N_{HW} \sim 24$. Thus, the effect of binding would become prominent for large strength h , and the protein is not foldable and stays in the denatured states with the values of $Q < 0.4$ [Fig. 2(g,h)]. Compared with the case with $h = 0.8$, we could conclude that the affinity-induced binding may compromise the confinement effect.

The folding rates K_f for various cavity sizes and affinity strengths are shown in Figures 3 and 4. Compared with the bulk case, the folding is fast for proper sizes when $L \geq 5$ and affinity strengths $h < 3.0$. This is controlled by both confinement and affinity: proper confinement would decrease the entropy of nonnative ensemble by suppressing the occurrence of loose coil states, and the weak affinity could reduce the difficulty to overcome the additional barrier on the free energy landscape due to the affinity-induced binding. Our simulation results support the previous study by Betancourt and Thirumalai using a simplified lattice model.¹³

More interestingly, due to the different nature of the confinement and the affinity, the folding rates show different behaviors as the values of cavity size and affinity strength change. For a fixed size of cavity, say $L = 6.0$, the folding rates change slightly when h is smaller than a certain strength $h' = 2.0$, but decrease fast when $h > h'$ (as shown in Fig. 3). For a weak affinity, the cavity wall cannot bind the protein steadily due to the thermal fluctuation, and the confinement dominates the folding, so the folding rate shows a weak dependence on h . Meanwhile, when $h > h'$, the effect of affinity takes on an important role. The rate exhibits a linear correlation with the affinity strength h as exhibited in Figure 3. In our simulations, this h' is approximately the same for most cases with different cavity sizes. Note that such a value of h' is related to temperature as it reflects the balance between the binding

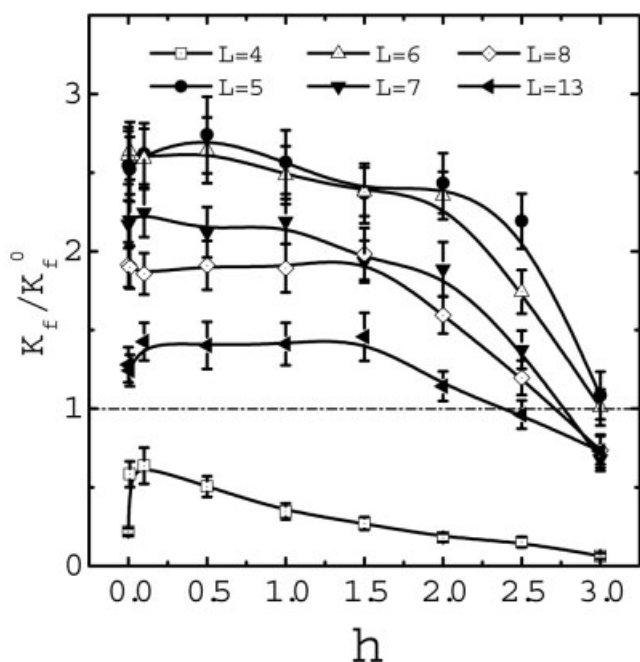


Fig. 3. Folding rate versus the affinity strength h for the chaperonin cavity with different radii L at T_f^0 . K_f is the chaperonin-mediated folding rate and K_f^0 is the folding rate in bulk.

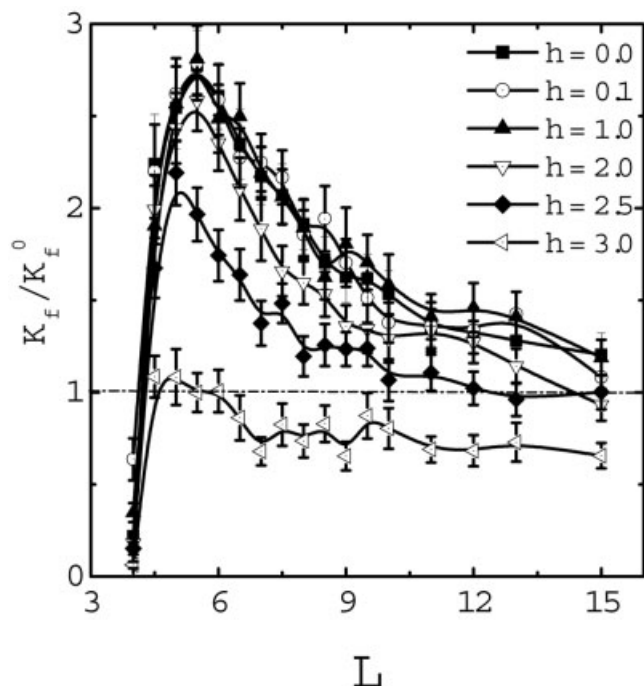


Fig. 4. Folding rate versus the radius L of the chaperonin cavity at different affinity strengths h at T_f^0 . K_f is the chaperonin-mediated folding rate and K_f^0 is the folding rate in bulk.

energy and thermal fluctuation. Another value of the affinity strength $h = 2.8$, defined as h_c , corresponds to the intersection when $K_f/K_f^0 = 1$, which marks the balance of confinement and affinity, just as the case shown in Figure 2(e). For cases with $h > h_c$, the chaperonin-associated

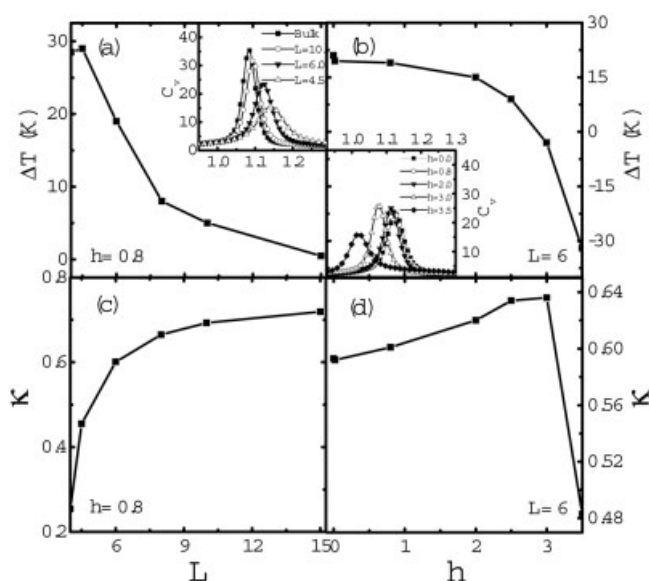


Fig. 5. The thermodynamic stability characterized by the difference between the folding transition temperature ($T_f - T_f^0$) and folding cooperativity κ versus the radius L of the chaperonin cavity and the affinity strength h . The inset in (a) is the heat capacity versus the temperature T for various radii of the cavity. The inset in (b) is the heat capacity versus the temperature T at various affinity strengths.

folding is slower than the case without chaperonin cavity. This kind of retardment has also been observed in previous experiments.^{36,37} Biologically, the ATP is often required to induce structural changes and decrease the affinity for releasing the substrate protein. On the other hand, for a fixed affinity, the variation of the folding rate is nonmonotonic and shows an optimization (see Fig. 4). Such optimization is also observed for cases in the absence of the affinity.^{33,35} The optimal L changes from 5.5 to 4.6 following the increase of h from 0 to 3.0. This is because the affinity-induced binding makes the nonnative protein being compact near the wall. Consequently, a small cavity may be suitable for the case with large affinity. For very large affinity, say $h \geq 3.0$, the affinity dominates the motion of the protein molecule and the confinement effect is largely weakened. Therefore, there is no apparent tendency of enhancement of the folding rate for these cases.

Thermodynamics of Folding

The variation of the thermodynamic stability of the substrate protein folding in the chaperonin system is also an interesting issue that has attracted many theoretical and experimental investigations.^{13,15,33-35,42} Here, the thermodynamic stability and cooperativity for the folding of the substrate protein in the chaperonin cavity are shown in Figure 5. The thermodynamic stability of the substrate protein is described by a difference $\Delta T = T_f - T_f^0$ between the folding transition temperature T_f in the cavity and T_f^0 in bulk. T_f is defined as the peak temperature of heat capacity. It is found that the value of ΔT clearly decreases as the cavity size increases [Fig. 5(a)] or the affinity

strength increases [Fig. 5(b)]. From Figure 5(a), we could conclude that the spatial confinement enhances the thermodynamic stability of the substrate protein. This is consistent with previous numerical,^{13,33} theoretical,³⁴ and experimental studies.^{31,32,78} In Figure 5(b), the value of ΔT changes from 21.2°C to -32.3°C when h changes from 0.0 to 3.5. It becomes negative when the affinity $h \geq h_c$, i.e., $h \geq 2.8$. These results indicate that the affinity between the protein and the chaperonin wall reduces the thermodynamic stability of the substrate protein. This is consistent with the experimental finding by Zahn et al.¹⁵ Interestingly, an affinity strength $h = 2.8$ where $\Delta T = T_f - T_f^0 = 0$ is consistent with the critical value observed from the kinetics, i.e., $h_c = 2.8$. Clearly, this is related to the cooperative feature of folding, and also shows the conjunction of thermodynamics and kinetics.

These results imply that the effect of the affinity is different from that of the spatial confinement for the folding of the substrate proteins. The nonspecific interactions induced by the affinity result in the attachment of residues on the chaperonin wall, and always work against the energetic bias for protein folding, rather than increase the bias as the spatial confinement does. Consequently, when $h > h_c$ (or $h < h_c$), the folding of the substrate protein could be considered to be dominated by the affinity (or the spatial confinement). However, the transition between these two kinds of folding modes is not very sharp, and could be considered as a crossover between each other. It is worth noting that the value of h_c depends on the cavity size (data not shown here).

In Figure 5(c,d), folding cooperativity κ of the substrate protein in the chaperonin cavity versus the cavity size L and the affinity h are shown. In Figure 5(c), the value of κ increases with the increase of the cavity size L . For the cavity size $L > 10$, the value of κ increases slowly and converges to the bulk case. The corresponding barrier in free energy landscape is high, so the folding cooperativity is high and the folding shows a good two-state behavior. As the cavity becomes small, the spatial confinement affects the folding and the barrier decreases. Since the confinement decreases the entropy of the denatured state ensemble, and destabilizes the denatured states, the cooperativity becomes low. This is consistent with the enhancement of the folding rate of the substrate protein with a strong spatial confinement. However, the cooperativity κ shows a nonmonotonic change as the affinity strength h increases [Fig. 5(d)]. When $h \approx 3.0$, the cooperativity reaches its maximum, and for larger h the cooperativity decreases sharply. Correspondingly, the peak height of the heat capacity increases when $h \leq 3.0$. Note that when $h \geq 3.5$, the peak height decreases since too strong an affinity keeps the protein attached on the chaperonin wall [see inset of Fig. 5(b)]. Clearly, for the folding in a hydrophobic chaperonin cavity, the binding of the substrate protein with the wall not only narrows the energetic distribution of the denatured states, but also increases the barrier of the transition on the free energy landscape. Thus, the protein would need to overcome a large barrier to reach the native state and the folding cooperativity is

enhanced. However, when the binding becomes too strong, the folding is difficult to achieve within a reasonable time since the protein molecule is tightly bound by the wall. In such a case, the folding cooperativity is deteriorated significantly.

To have some further insights, here, we calculate the profiles of the free energy by the WHAM algorithm⁷⁹ to analyze the effects of the confinement and affinity of the chaperonin cavity on the substrate protein folding. The probability distribution $P_T(Q)$ at a fixed temperature T was used to estimate the corresponding free energy $F_T(Q)$ ⁴⁴:

$$F_T(Q) = -\kappa_B T \log \frac{P_T(Q)}{P_T(Q_0)} + F_T(Q_0) \quad (7)$$

where Q_0 represents a reference state. We choose the native state as the reference state. From Figure 6(a), we can clearly see that the free energy profile for the folding of protein in bulk shows two minima located around the denatured states and the folded state at temperature T_f^0 , respectively. Then when the protein molecule is settled in the chaperonin cavity with various sizes at the same temperature T_f^0 , the free energy profiles become tilted toward the native state, i.e., there is a bias to the native state. The smaller the cavity size, the more bias to the native state the profile shows. This is attributed to the significant reduction of the conformational entropy of the denatured state with small size of the cavity. Obviously, such a bias suggests that the confinement may promote the folding of the substrate protein, as pointed out previously.^{13,33-35}

However, from Figure 6(b), it can be found that the bias of the free energy landscape is changed in reverse towards the denatured states as the affinity strength h increases. This can be interpreted as follows. The interactions induced by the affinity between the substrate protein and the chaperonin wall tend to bind the substrate protein and unfold it. In other words, there exists an unfolding process during the chaperonin-mediated protein folding and such a process becomes obvious when the affinity is strong. Therefore, the affinity gives the chaperone chances to behave differently, which may be reflected in different steps of the chaperone cycle.

The Unfolding Activity

The thermodynamics and kinetics of folding of the chaperonin-mediated unfrustrated protein show an interesting picture due to the concurrence of the spatial confinement and the affinity resulting from the cavity wall. In order to further characterize the folding processes of the substrate protein in the cavity in detail, we focus on the contacts formed between the hydrophobic residues and the chaperonin wall during the folding process (shown in Fig. 7). Unlike the case of protein in a hydrophilic chamber, the folding in the hydrophobic chaperonin cavity with a high affinity is slower than that in bulk. It is noted that this kind of process has been suggested to occur in cells.^{36,37} As the first step of the chaperonin-related protein folding process, does the chaperonin cavity play a positive role in the folding of the substrate protein?

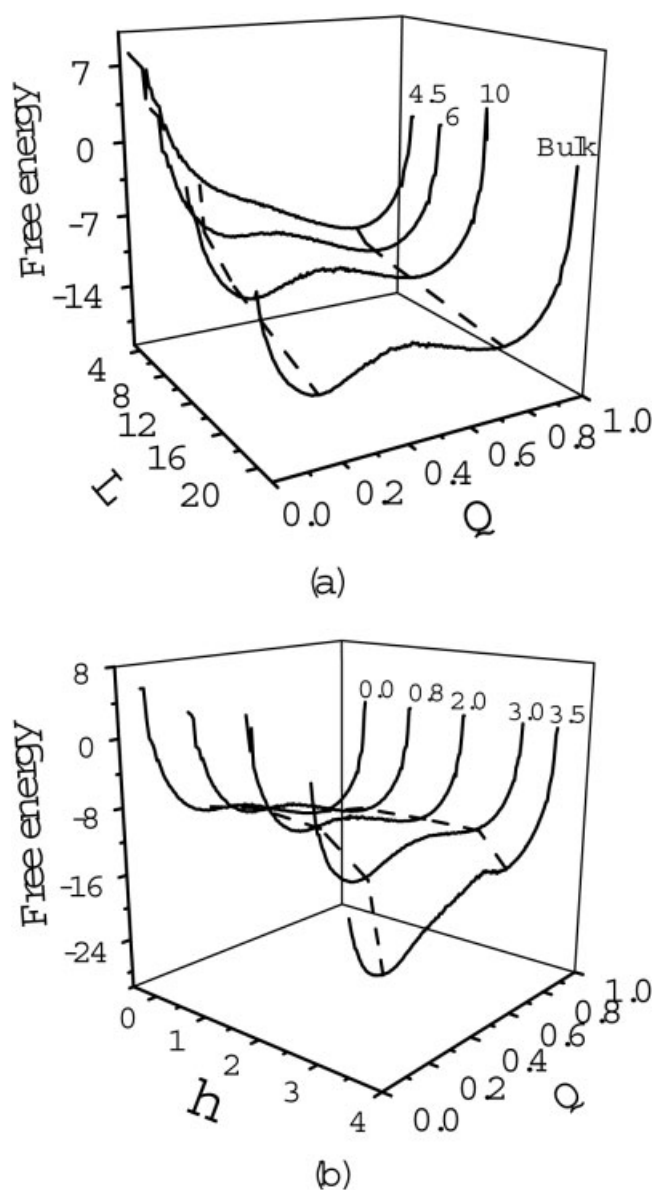


Fig. 6. The free energy profiles versus the reaction coordinate Q for the various cavity radii L (a) and affinity strengths h (b). All the simulations are performed at $T = T_f^0$.

Actually, when the affinity is strong enough, the confinement effect is relatively weak, that is, the enhancement of the folding rate due to the geometrical restriction is suppressed. This implies that the folding process in the cavity with strong affinity is governed by interactions between the hydrophobic residues and the chaperonin wall. The number of contacts N_{HW} formed between the substrate protein and the chaperonin wall and the number of nonnative contacts N_{HH} formed between the hydrophobic residues of the substrate protein themselves during the folding process may be proper indicators for characterizing the folding process. Here the averaged numbers N_{HW} and N_{HH} are studied, and are obtained by averaging N_{HW} and N_{HH} over a time period before the protein becomes folded. Figure 7 shows that the averaged number N_{HW} becomes

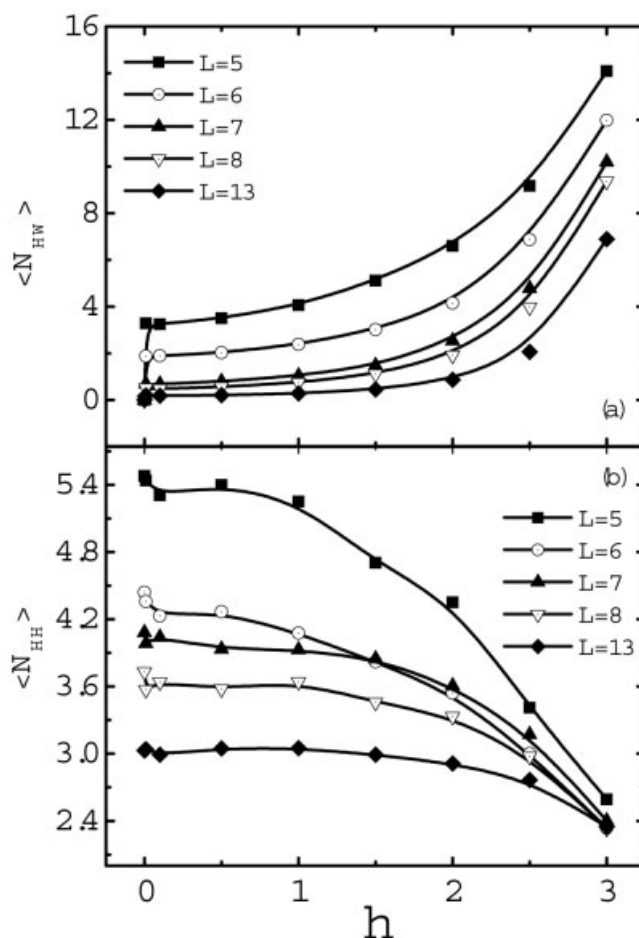


Fig. 7. The average number of contacts formed between the hydrophobic residues and the chaperonin wall N_{HW} (a), and the average number of nonnative contacts formed between the hydrophobic residues N_{HH} (b) at different cavity radii L during the folding process. The average is over 100 trajectories at $T = T_f^0$.

larger, whereas the averaged number N_{HW} becomes smaller as the affinity strength h increases for various cavity sizes. This reverse change of N_{HW} and N_{HH} during the folding process is observed, suggesting that the affinity destabilizes the packing of hydrophobic residues. In this sense, the contacts formed between the substrate protein and the chaperonin wall significantly reduce the probability of forming the nonnative contacts between the hydrophobic residues and some nonnative traps are cleaned up.

In addition, it is noted that the smaller the cavity size is, the more the number of contacts N_{HW} and N_{HH} are formed. For example, for the case of cavity with $L = 13$, there is basically no contact between the protein and the wall and only 3 nonnative contacts between hydrophobic residues when $h < 2.0$. When $L = 5.0$, the number of contacts N_{HW} is about 4 or 6 and the number of contacts N_{HH} is about 4.5 or 5.4. Furthermore, when $h > 2.0$, the value of N_{HW} increases rapidly, but the value of N_{HH} decrease rapidly. In the case of $L = 5.0$ and $h = 3.0$, about 14 contacts are formed between the substrate protein and the wall, which takes about 46.7% of the total hydrophobic residues. About

2.7 nonnative contacts are formed between hydrophobic residues, which takes about 9% of the total hydrophobic residues.

Therefore, in step 1 of the chaperonin-related protein folding process, the affinity of the chaperonin cavity plays an important role in destabilizing the unfolded or misfolded states. The folding in this kind of environment starts generally from an unfolding process. Consequently, the whole folding process could be regarded as a serial process with binding (destructing) and then folding. However, the binding with the chaperonin wall imports some additional energetic frustrations, which make the folding even slower than that in bulk. Actually, in this step the chaperonin cavity prepares an unfolded environment for the next step (folding), namely a hydrophilic wall after allosteric transition of the chaperonin. This also offers a possible explanation to the unfolding processes of the IAM.²⁸ This kind of unfolding processes is also consistent with the variation of thermodynamic features.

In the phenomenological working cycle for the chaperonin-associated folding of the substrate protein, the affinity of the cavity may behave as a change from strong hydrophobicity to weak hydrophobicity and then back to strong hydrophobicity again. This can be modeled in our simulations by just changing the affinity strength. Here we show two examples of the folding process for the protein molecule in a cavity when the affinity is switched between a strong hydrophobicity $h = 3.0$ and a weak hydrophobicity $h = 1.0$. The cases of $h = 3.0$ and $h = 1.0$ are referred to as the step 1 and the step 2 of the working cycle, respectively. We divide the time period of the cycle t_c into t_p during which the wall is weak hydrophobic (P) and $(t_c - t_p)$ during which the wall is strongly hydrophobic (H). The time evolution of the number of contacts between the residues and the wall N_{HW} and the nonnative contacts between hydrophobic residues is illustrated in Figure 8(b,e). The corresponding distributions of the contacts are also shown in Figure 8(a,c,d,f), respectively. From Figure 8(b), it is clearly seen that the values of N_{HW} are large, but the values of N_{HH} are comparatively small when the affinity strength is $h = 3.0$ during the time period $t_c - t_p$. Correspondingly, from the distributions of two kinds of contacts shown in Figure 8(a), one can find that the values of N_{HW} show a wide distribution from $N_{HW} = 2$ to 22 and most of the values are around $N_{HW} = 10$. Differently, the values of N_{HH} show a sharp distribution around $N_{HH} = 1$ to 5. This indicates that the protein is bound to the cavity wall. In contrast, when the affinity strength is decreased from $h = 3.0$ to 1.0, the results are reversed. The values of N_{HW} decrease significantly, but the values of N_{HH} increase distinctly, which is obviously exhibited in the distributions of two kinds of contacts as shown in Figure 8(c). When h is changed from 1.0 to 3.0, a reverse process can be observed as presented in Figure 8(e). These are attributed to the fact that large numbers of contacts are formed between the substrate protein and the chaperonin wall as the affinity is strong, which restrains the formation of the nonnative contacts between the hydrophobic residues. As the affinity is weak, the affinity takes almost no effect and more

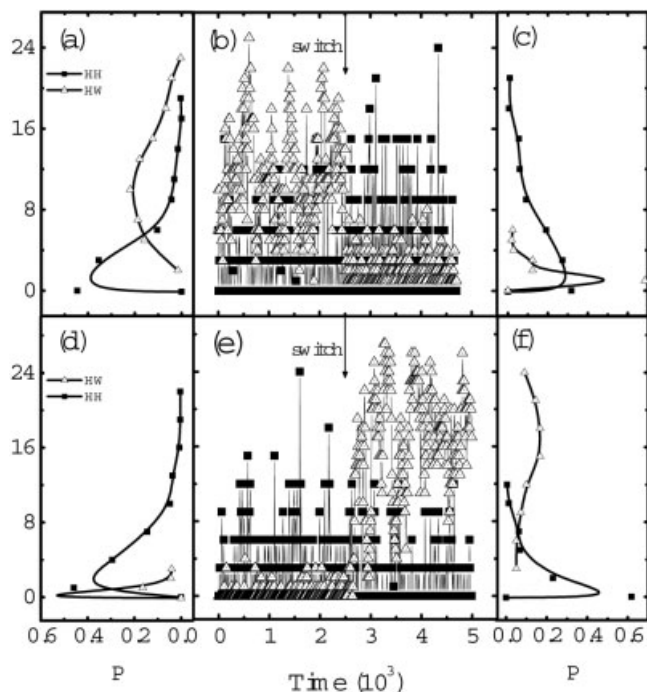


Fig. 8. The number of contacts formed between the residues themselves of the substrate protein (denoted by solid squares) and the number of contacts formed between the substrate protein and the chaperonin wall (denoted by open triangles) plotted as a function of time for the chaperonin within a hydrophobic cycling. The hydrophobicity is changed from $h = 3.0$ to $h = 1.0$ (b) and from $h = 1.0$ to $h = 3.0$ (e). The cycling time is set to 10^6 MD step, the simulation temperature is at $T = T_f^o$, and the cavity radius is $L = 6$. a, c, d, f: The corresponding frequency counts for the related contact numbers. The arrows in b and e indicate the onset time of the switch on the affinity.

nonnative contacts are formed between the hydrophobic residues. Therefore, following the switching of the cavity environment, the weights of two kinds of contacts for the protein would change consequently. This illustrates that the affine environment prefers the contacts between the substrate protein and the chaperonin wall.

In addition, in order to observe the conformational changes arisen from the hydrophobic cycling, we study the structural features right before and after the change in the chaperonin hydrophobicity. In Figure 9, the distributions of the root mean square of distance (RMSD)⁸⁰ are shown for the cases before and after the transition from $h = 3.0$ to $h = 1.0$ [Fig.9(a)] and from $h = 1.0$ to $h = 3.0$ [Fig.9(b)], respectively. The RMSD describes the similarity of a certain conformation to the native state of the protein. The smaller the value of the RMSD, the more similar the conformation to the native state. In Figure 9(a), when $h = 3.0$, many hydrophobic residues are tightly bound to the chaperonin wall and the substrate protein is unfolded. Thus, the values of RMSD are large and are distributed around 2.5. However, when h is decreased to 1.0, those residues that are in contact with the chaperonin wall are released from the wall, and the substrate protein resumes the folding. Therefore, the distribution of the values of the RMSD is shifted to the low value region with a peak around 1.6. This indicates that the substrate protein is

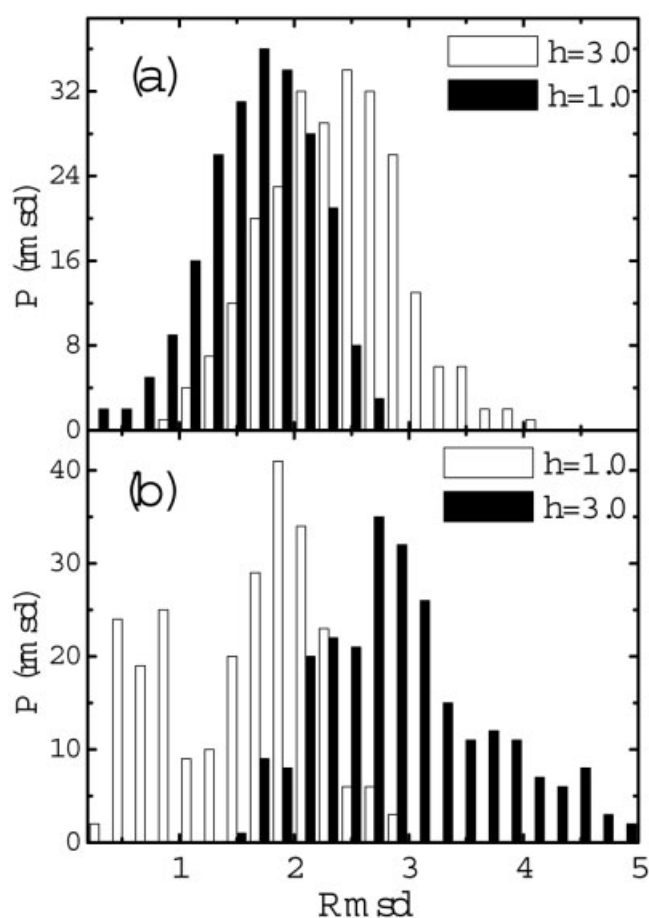


Fig. 9. The conformational changes characterized by the distributions of the root mean square of distance (RMSD) during the switch of the affinity of the cavity related to Figure 8. The distribution is calculated before and after the hydrophobicity is changed from $h = 3.0$ to $h = 1.0$ (a) and from $h = 1.0$ to $h = 3.0$ (b).

given another chance to fold to its native state when the affinity strength is changed from strong to weak.

Nevertheless, we can see the reverse process in Figure 9(b) when the affinity strength is changed from $h = 1.0$ to $h = 3.0$. When $h = 1.0$, the effect of affinity is negligible and the confinement drives the folding of the substrate protein. Thus, the values of the RMSD are small. However, when h is increased to 3.0 from 1.0, the substrate protein is tightly bound by the chaperonin wall and is unfolded. The distribution of the values of the RMSD is shifted to the high value region, indicating that the chaperonin cavity acts as an unfoldase when the affinity is strong. This unfolding activity of the substrate protein due to the changes in the hydrophobicity of the cavity was first studied by Betancourt and Thirumalai via observation on the χ -values, which describes the inherent structure of the protein chain.¹³ Such a picture is in accord with the IAM mechanism.²⁸ These also are consistent with our previous results. Thus, we can draw a conclusion that the affinity-induced interactions between the substrate protein and the chaperonin cavity play a positive role in chaperonin-mediated protein folding. In step 1 of the chaperonin cycle,

the substrate protein is first tightly bound by the GroEL molecule, and, at the same time, the interactions between them induce an unfolding and eliminate the kinetic traps or the misfolded states. Therefore, the interactions facilitate the whole folding process.

How Does the Chaperonin Wall Affect the Folding?

The interactions between the substrate protein and the chaperonin wall affect both the thermodynamics and kinetics of the folding. In order to probe how the affinity of the chaperonin wall affects the folding features of the substrate protein, we made some mutations on the protein. Our results suggest that the binding of the inner hydrophobic residues with the chaperonin wall seems to play a more important role than the exterior hydrophobic residues do during the folding of the substrate protein. In addition, the decrease of the number of the hydrophobic residues enhances the folding rate when the affinity is strong.

Different roles of exterior and inner hydrophobic residues of the substrate protein

From the analysis on the thermodynamics and kinetics of folding, it is easy to find that the binding of hydrophobic residues with the chaperonin wall is unfavorable for the formation of the protein structure, and thus obviously retards the folding. However, it is not clear whether this kind of nonspecific interaction makes all the hydrophobic residues contribute equally to the folding process. The answer to this question would be instructive for understanding how the affine wall affects the folding of substrate proteins. As a simple approach, we build two model chains, each of which have only half numbers of H-type residues of the original substrate protein. One sequence keeps the internal H-type residues, and the other preserves the surface H-type ones. The determination of insiderness/outsiderness is based on the solvent exposure. Here, the inner hydrophobic residues are defined for those with solvent exposure $<20\%$, and the exterior hydrophobic residues with solvent exposure $>20\%$.⁸¹ The solvent exposure of residues is calculated using the program MOLMOL.⁸² These two chains are named HI-chain (with hydrophobic residues inside) and HS-chain (with hydrophobic residues on the surface), respectively. It is noted that the alteration of these hydrophobic residues only affects the interactions with the chaperonin wall, not the interactions intra-protein. From Figure 10, one can see that the folding behaviors of the HI-chain and HS-chain are somewhat different. The folding rate of the HI-chain is slower than that of the HS-chain around the optimal chaperonin cavity sizes, i.e., around $L = 5.5$. This implies that the inner hydrophobic residues have more effect on the folding rate than the exterior hydrophobic residues have though the interactions of both kinds of residues with the wall are in the same level of magnitude. The reason could be given in the following way. Obviously, the inner hydrophobic residues are surrounded by other residues. Thus, the binding of the inner hydrophobic residues with the chaperonin wall may prohibit the formation of the local structures of these hydrophobic residues due to the steric restriction.

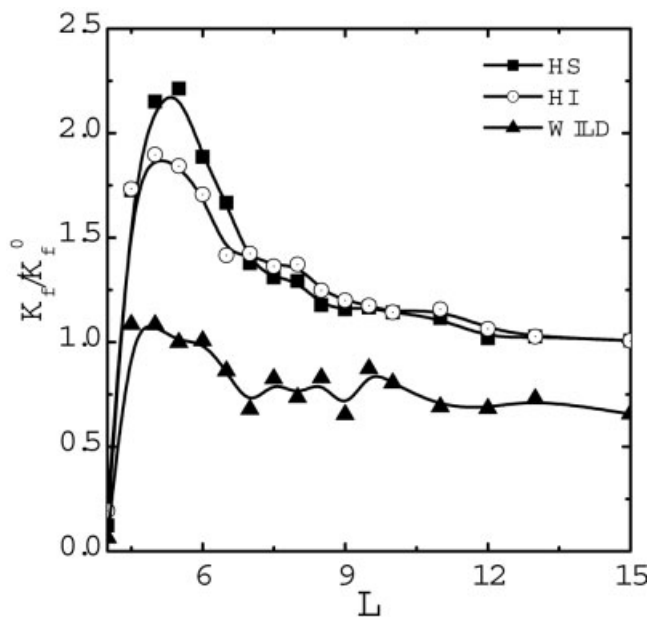


Fig. 10. The folding rate K_f^b/K_f^c versus the cavity radius L for three chains. The solid squares marked with "HS" correspond to a case in which all the inner hydrophobic residues are mutated. The open circles marked with "HI" correspond to a case in which all the mutated residues are located at the exterior of the protein. The solid triangles marked with "WILD" correspond to the wild type protein. All the simulations are performed in the chaperonin cavity with the same affinity strength $h = 3.0$ at T_f^0 .

However, for the hydrophobic residues on the surface, the binding with the wall has less effect on the formation of the local structure since those residues in contact with the wall are regularly distributed on the surface with almost fixed orientation related to their neighboring residues. In fact, the interactions between the exterior hydrophobic residues and the chaperonin wall could still exist even though the protein has been folded successfully. It has been observed in an experiment that the native barnase binds weakly to the GroEL with a dissociation constant in the mM region.⁸³ In such a sense, the inner residues and the residues on the surface of the substrate protein do not contribute equally to the folding processes. These are relevant to previous experimental observations.³⁷

Clearly, the decrease in the number of hydrophobic residues always increases the folding rate with respect to the folding of the wild-type chain as shown in Figure 10. This indicates that the binding of both the inner hydrophobic residues and the exterior hydrophobic residues with the chaperonin wall affects the folding kinetics of the substrate protein. However, the hydrophobic residues on the surface of the substrate protein play a less important role in affecting the folding kinetics compared with the inner hydrophobic residues.

Folding in the chaperonin cavity after point mutation of the substrate protein

To further study the importance of the affinity between the chaperonin wall and the substrate protein and the roles of the exterior and inner hydrophobic residues in the

chaperonin-mediated protein folding, we performed simulations of the folding of protein chymotrypsin inhibitor-2 with point mutation on some sites, in comparison with the available experimental results.³⁷ Each mutation is implemented by changing the hydrophobic residue at a certain site to a hydrophilic one, and at the same time all the related contacts are removed. In our simulations, the selection of mutational sites refers to previous experiments³⁷ and a total of 15 hydrophobic residues of protein CI2 are mutated, respectively.

Both the cases in the presence and absence of the chaperonin cavity are studied for comparison. For various mutants, it is found that the folding rates in bulk decrease with respect to the case of the wild-type, and the folding is further retarded in the presence of the chaperonin cavity (see Table I, where K^c and K^b represent the folding rates in the presence of the chaperonin and in bulk, and the subscript index T or E is used to indicate theoretical simulations or the experiments, respectively). However, the variation of the folding rates in the presence of the chaperonin are not the same as those of the bulk cases since the mutations weaken the interactions between the substrate protein and chaperonin, which may promote the folding in some degree. This difference in variation of folding rates suggests that the interactions are actually one of the important factors in chaperonin-assisted protein folding processes. These are qualitatively consistent with the experimental results by Itzhaki et al. in which it is shown that the folding rate of CI2 in GroEL does not appear to be as sensitive to mutation as the folding rate in solution.³⁷ Actually, the change of folding rate results from both effects of mutations on stability and of the chaperonin cavity. In order to characterize the effect of affinity between the substrate protein and the chaperonin cavity on kinetics, we use a factor K^b/K^c . The larger the value of K^b/K^c , the more significant the effect of the affinity is. It has been found that our simulation results K_f^b/K_f^c correlate well with the experimental results K_E^b/K_E^c obtained by Itzhaki et al.³⁷ with a correlation coefficient $R = 0.826$ as shown in Figure 11. Note that the correlation between the folding rate K_T^b (or K_T^c) and K_E^b in bulk (or K_E^c in the chaperonin cavity) is weaker with correlation coefficients $R = 0.31$ and 0.58 .

From Figure 11, it is noted that the values K^b/K^c for the mutant A16G is quite large, while for the mutants L49A and I29A/I57V the values are small for both the cases of experiments and simulations (note that our residue numbering is 1–64, rather than 20–83). This seems to be abnormal since site 16, which has been identified as the folding nucleus site,⁸⁴ is an inner hydrophobic residue and ought to have a significant effect on the folding kinetics according to our previous conclusion. That is, the mutant A16G should induce a small value of K^b/K^c similar to the cases of mutant L49A and I29A/I57V. Here sites 49 and 57 are also folding nuclei and inner hydrophobic residues.⁸⁴ A detailed study on the structural features of the protein gives us an interpretation for the difference. It is found that site 16 is located in the α -helix (residues 12–24) and is surrounded by the N-terminal coil and three strands of

TABLE I. Rate Constant of Refolding of CI2 in Bulk and in GroEL Cavity

Mutant	$K_T^b(10^{-4}r^{-1})$	$K_T^c(10^{-4}r^{-1})$	$K_E^b(s^{-1})$	$K_E^c(s^{-1})$
Wild	2.63 ± 0.20	0.45 ± 0.03	56.8 ± 2.50	1.82 ± 0.01
L8A	1.52 ± 0.11	0.31 ± 0.02	28.8 ± 1.10	1.66 ± 0.03
A16G	2.44 ± 0.18	0.38 ± 0.03	8.10 ± 0.20	0.37 ± 0.06
I20V	0.57 ± 0.05	0.23 ± 0.01	23.6 ± 0.60	1.85 ± 0.04
L21G	2.33 ± 0.16	0.42 ± 0.03	25.2 ± 0.70	1.25 ± 0.02
I29A/I57V	0.40 ± 0.03	0.23 ± 0.01	7.60 ± 0.30	1.45 ± 0.05
I30A	1.33 ± 0.10	0.39 ± 0.01	18.9 ± 0.90	4.50 ± 0.15
L32A	1.04 ± 0.09	0.37 ± 0.02	26.7 ± 3.00	3.33 ± 0.02
L32A/F50A	0.32 ± 0.02	0.22 ± 0.01	6.3 ± 0.60	1.90 ± 0.02
Y42G	1.89 ± 0.18	0.48 ± 0.02	43.2 ± 1.20	3.66 ± 0.01
L49A	0.50 ± 0.04	0.24 ± 0.01	1.80 ± 0.10	0.18 ± 0.02
V51A	1.25 ± 0.11	0.33 ± 0.02	24.6 ± 0.90	2.00 ± 0.06
A58G	2.33 ± 0.16	0.40 ± 0.03	39.5 ± 0.90	1.97 ± 0.06
V60G	1.21 ± 0.10	0.31 ± 0.02	45.8 ± 1.20	1.87 ± 0.03
F50A	0.44 ± 0.03	0.25 ± 0.01	10.1 ± 0.01	1.04 ± 0.04
V38A/F50A	0.37 ± 0.02	0.23 ± 0.01	7.50 ± 0.30	2.00 ± 0.04

^bRate constant for folding of CI2 in bulk.

^cRate constant for folding of CI2 in GroEL cavity.

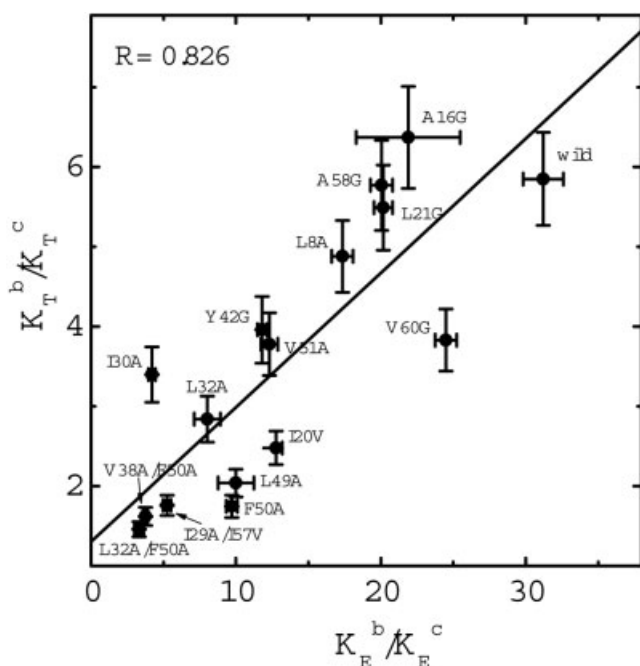


Fig. 11. The correlation between our simulation results of K^b/K^c and those obtained experimentally by Itzhaki et al.³⁷ and the correlation coefficient is $R = 0.826$. The simulation temperature is set as $T = 1.052$, which is the folding transition temperature in bulk. The affinity strength is set as $h = 3.5$. The error bar is calculated with the error recursion formula for divisions. The related mutations are also marked.

β -sheet (residues 11–13, 28–34, 55–58). The residues 16, 29, 49, and 57 form a hydrophobic cluster. The residue 16 plays a key role in the contact network, which connects the α -helix and three strands of β -sheet mentioned above. Once this hydrophobic residue A is mutated to a hydrophilic residue G, the connection of the contact network may be severely destroyed, and the inner hydrophobic residues will be exposed to the chaperonin wall. This retards the folding in the cavity, i.e., a decrease in the

value of K^c . Therefore, the value of K^b/K^c increases. Nevertheless, for sites 49 and 57, their mutants will not produce a large effect due to their structural features. The residues 49 and 57 are all wrapped by other secondary structures. The mutation of the residues 49 or 57 to hydrophilic residues will only reduce the binding between the protein CI2 and the wall of the chaperonin cavity. Thus, the folding of protein CI2 in the cavity is enhanced, i.e., the value of K^c increases, so the value of K^b/K^c is small.

Itzhaki et al. have experimentally studied the refolding process of CI2 mediated by GroEL and obtained many other significant results. Here, following their procedures, by simulation, we try to further illustrate the same behavior of the chaperonin-mediated protein folding. Although GroEL is not biologically required for the folding of CI2, it is helpful to investigate its refolding process mediated by the chaperonin. This could provide significant insights into the important role of chaperonin-protein interactions. Here, we examine the change in binding affinity on mutation, which is expressed in terms of the Eq.(5) in the report by Itzhaki et al.³⁷ Consistent with the experimental analyses by Itzhaki et al., our simulation results also show that the change of hydrophobic residues to hydrophilic ones weakens the binding between the chaperonin cavity and protein CI2 (see Fig. 12). Apart from this, we especially study the relation between the strength of the binding interactions and the folding rate for CI2 by referring to the idea by Itzhaki et al.. The change of binding affinity $-RT \ln(K_T^b/K_T^c)$ as a function of the difference in free energy of transfer of the wild-type and mutated side chain from n-octanol to water is shown in Figure 13. The values of the free energy difference are calculated based on the data obtained by Hansch and Leo,⁸⁵ using the equation:

$$\Delta G_{transfer(n-octanol-water)} = RT(\pi_{wildtype} - \pi_{mutant}), \quad (8)$$

where $\pi = \log P$ and P is the partition coefficient of the mutated side chain between water and n-octanol. Inspir-

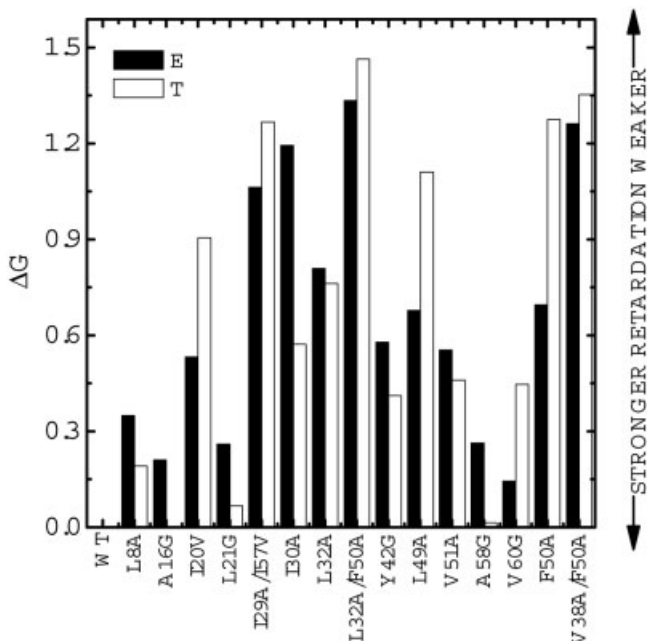


Fig. 12. Relative retardation of folding on binding of different mutants of C12 to the chaperonin cavity. The letter "T" denotes that the results are obtained by simulation and the letter "E" represents those gained from experiment.

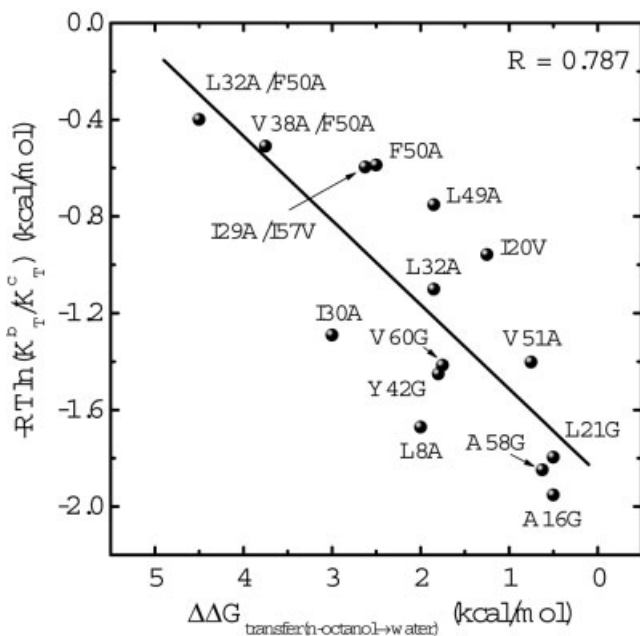


Fig. 13. The correlation between the change of binding affinity $-RT\ln(K_T^b/K_T^c)$ and the free energy difference of transfer of the wild-type and mutated side chain from *n*-octanol to water $\Delta\Delta G_{\text{transfer}(n\text{-octanol}\rightarrow\text{water})}$. The correlation coefficient is $R = 0.787$.

ingly, an obvious correlation between the free energy difference $\Delta G_{\text{transfer}(n\text{-octanol}\rightarrow\text{water})}$ and the change of binding affinity $-RT\ln(K_T^b/K_T^c)$ is found for the mutants with a correlation coefficient $R = 0.787$. As argued by Itzhaki et al., a small slope in Figure 13 indicates that only a fraction of the hydrophobic energy is lost on going from the bound

denatured states to the transition state. The negative slope of the plot means that the relative rates of folding are inversely correlated with the strength of the binding interactions. That is, the weaker the binding, the faster the folding. Thus, the folding of the GroEL-complexed CI2 involves the breaking of hydrophobic interactions between the chaperonin and protein CI2. This further shows that the change in the hydrophobic interactions affects the folding rate of the encapsulated CI2, suggesting an important role played by the binding interaction.

As another illustration of different effects of the inner hydrophobic residues from the exterior hydrophobic residues on affecting the folding kinetics, we probe the whole effect of the inner hydrophobic residues and the exterior hydrophobic residues by calculating the average value of the factor K_T^b/K_T^c . Interestingly, the average value of the factor K_T^b/K_T^c is 3.1 for the inner hydrophobic residues, while that for the exterior hydrophobic residues is 4.7. Correspondingly, the related experimental values are 12.5 for the inner hydrophobic residues and 14.1 for the exterior hydrophobic residues.³⁷ Note that the average value of K_T^b/K_T^c for the inner hydrophobic residues is smaller than that for the exterior hydrophobic residues. This has the same relationship for those obtained from the experiments. However, the values from our simulations are one third of the experimental ones, which may result from the simplified Go-type interactions since the funnel-like landscape is smoothened. Anyhow, our simulation results are qualitatively consistent with the experiment, showing that, in general, the mutations of the inner hydrophobic residues to polar type could induce a larger effect on the folding kinetics of protein CI2. This further verifies the roles of various residues in the folding in the chaperonin cavity and is consistent with our conclusion in "How Does the Chaperonin Wall Affect the Folding?" that the inner hydrophobic residues play a more important role than the exterior hydrophobic residues in the interactions with the chaperonin wall. This also suggests that the affine wall plays a role in affecting the folding pathway. The affine wall blocks the folding when the inner hydrophobic residues are bound with the wall. These inner hydrophobic residues might be related to the wrong folding. At the same time, the affine wall has weak effects on the folding with correct packing, i.e., the protein collapses quickly and the inner hydrophobic residues are settled inside correctly. Thus, the chaperonin system with an affine wall plays a role to alter the pathways of the folding on the landscape. Our results indicate that the interactions between the residues and the chaperonin wall are indeed the important reason to dominate the folding in the chaperonin system. Especially, the affinity is important for modeling the chaperonin system, and, by considering the affinity between the substrate protein and the wall of the cavity, our chaperonin model can well describe the real situation of the chaperonin-mediated protein folding.

CONCLUSIONS

The folding of substrate proteins in chaperonin cavity is an interesting and not very clear topic. Previously, some

experimental studies showed that the chaperonin system could enhance the folding rate of the substrate proteins, while others found that the chaperonin system retards the folding. In the present report, we study the folding process of the chaperonin-mediated substrate protein by considering the effects of affinity and confinement. Furthermore, based on simulations using the G \bar{o} -type model, which has been widely used in the modeling on protein folding in recent years, we propose a possible mechanism for the chaperonin-mediated protein folding, which provides an understanding of the puzzle of protein folding *in vivo*.

We used a simplified representation for both the substrate protein and the chaperonin system. In our model, the nonspecific hydrophobic interactions between the hydrophobic residues are included, which does not alter the native state of the protein. Thus, the model protein is unfrustrated, and at the same time the interactions between the hydrophobic residues of the substrate protein and the chaperonin cavity are considered. Although simple, such a model helps us to capture the basic physical features of the chaperonin-mediated protein folding. For the substrate protein, we focus on two α/β sandwich proteins, namely the protein Ada2h and CI2, which belong to a common structural motif found in the GroEL substrate proteins. The folding with a single binding event is considered, and the real cycle process is also included. Moreover, a significant native-like structure does exist in protein-folding intermediates bound to the GroEL, which are in accord with the experimental observations.^{8,69,70,86} We find that when the affinity between the substrate protein and the chaperonin wall is weak, this chaperonin-mediated process enhances the folding rate of the substrate protein compared with that in bulk. In this case, the confinement plays an important role. However, if the affinity is strong enough, the substrate protein is nonspecifically bound by the chaperonin and partly unfolded. Thus, the folding is retarded. This agrees well with the experimental findings that there is an inverse correlation between the strength of the hydrophobic interactions and the rate constant for refolding of the GroEL-complexed protein.³⁷ In such a case, the affinity-induced kinetic effect plays a main role in folding. The strong hydrophobic environment may be unfavorable to the folding of the unfrustrated protein. Nevertheless, it may be favorable to the folding of the highly frustrated protein. This is attributed to the fact that for the frustrated protein the binding between the substrate protein and the chaperonin cavity could make the frustrated protein be unfolded. Such unfolding provides the protein more chances to escape from the kinetic trapping and then enables the protein to fold correctly, leading to an overall acceleration in the folding rates. Recently, it was demonstrated that a moderately hydrophobic environment, similar to the interior of the GroEL cavity when bound with ATP and GroES, is sufficient to accelerate the folding of a frustrated protein.^{13,18,39,40}

Therefore, our model may provide a possible mechanism to understand the diversely experimental phenomena. It is well known that the barrier of folding results from two

kinds of sources, namely energy and entropy. When energy is rather optimized, the barrier is mainly caused by the entropic effect. This has been argued as the minimal G \bar{o} -model (Type I). When there are some apparent intermediates in folding pathways, the activation from the energetic traps is more important, such as Shea's modified HT mode¹⁸ (Type II). The chaperonin cavity with affinity affects the energy and entropy during the folding of the substrate protein simultaneously. It decreases the entropy of the extended denatured states, and also stabilizes the states bound with the wall. These states are generally denatured too. For the cases of weak affinity, it is easy to understand that the confinement effect of the cavity on the entropy is somewhat dominant. For type-I model proteins, this will destabilize the denatured states, which enhances the folding rate as shown in our work. However, for the type-II model proteins, the confinement has less effect on the compact intermediates, and the binding with the cavity wall stabilizes the intermediates. This results in proteins folding slowly. In the case of stronger affinity, the energetics takes a main role. For type-I model proteins, the decrease of energy balances or even exceeds the effect of confinement. Thus, the barrier is higher, resulting in a slow folding as found in our work. In contrast, for type-II model proteins, the implicit unfolding (namely pulling the protein from intermediates to extended denatured states by bias from binding) may increase the folding rate as argued in previous studies.^{14,18,28} As a matter of fact, findings in previous studies⁸⁷⁻⁹¹ have shown that ATP can modulate the strength of affinity (in general, reduces the affinity) and the folding could be reactivated when ATP is introduced.

The unfolding process caused by affinity is also probed in our work. Interestingly, the unfolding process will significantly break the mis-formed nonnative hydrophobic contacts. This affinity-induced unfolding process destabilizes the substrate protein, which is reflected by the reduction of the folding temperature found in our simulations. Zahn et al. also observed a reversible lowering of the melting temperature of barnase in the presence of the GroEL in their experimental work.¹⁵ Thus, we believe that the chaperonin cavity has at least two functions in the chaperonin-mediated protein folding: the functions of spatial confinement and kinetic unfolding. Moreover, by checking the role of the hydrophobic residues playing in the interactions with the hydrophobic chaperonin wall, we find that the buried inner hydrophobic residues have a more significant effect on the folding than the exterior ones.

In addition, the folding features for the various mutants of protein CI2 have been studied further. Inspiringly, our simulation results on the folding rates show a good correlation with the experimental results obtained by Itzhaki et al.³⁷ Consistent with the experimental analyses, the simulation results also show that the change of hydrophobic residues to hydrophilic ones weakens the binding between chaperonin cavity and protein CI2. And the relative rates of folding are inversely correlated with the strength of the binding interactions: the weaker the binding, the faster the rate of folding. This further testifies that our model of

the chaperonin cavity is valid in the investigation of the chaperonin-mediated protein folding. The chaperonin cavity with an affine wall plays an important role in changing the folding pathways on the landscape. This suggests that the interactions between the residues and the chaperonin wall are, indeed, one of the main reasons dominating the folding in the chaperonin system. At the same time, our results indeed confirm our conclusion that the buried inner hydrophobic residues and the exterior hydrophobic residues play different roles in the folding of the chaperonin-mediated proteins.

Finally, it is worth noting that the hydrophobic interactions are nonmonotonically dependent on temperature.^{92–94} In our work, this temperature dependence of folding behaviors was also cursorily studied. Simulations on folding kinetics at a series of temperatures were performed. The results were qualitatively similar to those obtained at T_f^0 (results not shown), although hydrophobic interactions are temperature dependent.^{92–94} This could be attributed to the enhancement of the stability due to confinement. In fact, the temperature factor is implicitly included in the parameter of affinity strength (h) in our model. It is found that the folding of the substrate protein would be enhanced by the chaperonin at different h as long as $h < 3.0$. That is, confinement plays a key role in assisting the folding of substrate proteins under different temperature conditions. This is consistent with the wide range of working temperatures of chaperonin. Also, the effect of affinity somehow can be weakened at high temperature, which may be partly helpful for the release of substrate protein when the energy of ATP is imported. However, the detailed effects of temperature on the chaperonin-assisted protein folding due to the dependence of hydrophobic interactions on temperature are quite complicated and still unclear. This is a topic that deserves to be studied in our future work.

It is also valuable to note that the current model might be generalized to more realistic cases of protein folding in vivo, such as folding in chaperonin systems including more features of the chaperonin and folding concerning effects of macromolecular crowding in cells. In a more realistic chaperonin cavity, interactions may only exist between certain regions of the chaperonin cavity and substrate proteins. The affinity strength may be variable during the processes of chaperonin-mediated protein folding and may also relate to the conformational change of the chaperonin cavity. These can all be further investigated with an extended version of our current model. It is well known that the folding in vivo is more complicated than that in vitro due to the crowded and intricate environment including different kinds of macromolecules in cells. Based on the effective concentration of protein molecules, the folding of the protein chain can be confined within a related size of cavity. Such a cavity should be optimized and can be modeled with different geometrical shapes. At the same time, the interactions between the object protein and other macromolecules could be mimicked as the affinity under proper consideration. Some significant phenomena, such as protein aggregation, amyloid fibril formation, and so on,

relevant to macromolecular crowding and/or interactions between the molecules could be studied by incorporating certain specific interactions with the general volume exclusion effect of the confinement. These are of great interest and might be implemented with our current model.

ACKNOWLEDGMENTS

J. Wang thanks the support of FANEDD.

REFERENCES

1. Dill KA, Chan HS. From Levinthal to pathways to funnels. *Nat Struct Biol* 1997;4:10–19.
2. Leopold PE, Montal M, Onuchic JN. Protein folding funnels: a kinetic approach to the sequence-structure relationship. *Proc Natl Acad Sci USA* 1992;89:8721–8725.
3. Bryngelson JD, Onuchic JN, Socci ND, Wolynes PG. Funnels, pathways, and the energy landscape of protein folding: a synthesis. *Proteins* 1995;21:167–195.
4. Onuchic JN, Wolynes PG, Luthey-Schulten Z, Socci ND. Toward an outline of the topography of a realistic protein-folding funnel. *Proc Natl Acad Sci USA* 1995;92:3626–3630.
5. Wolynes PG, Luthey-Schulten Z, Onuchic JN. Fast-folding experiments and the topography of protein folding energy landscapes. *Chem Biol* 1996;3:425–432.
6. Onuchic JN, Luthey-Schulten Z, Wolynes PG. Theory of protein folding: the energy landscape perspective. *Annu Rev Phys Chem* 1997;48:545–600.
7. Nymeyer H, Carcía AE, Onuchic JN. Folding funnels and frustration in off-lattice minimalist protein landscapes. *Proc Natl Acad Sci USA* 1998;95:5921–5928.
8. Martin J, Hartl FU. The effect of macromolecular crowding on chaperonin-mediated protein folding. *Proc Natl Acad Sci USA* 1997;94:1107–1112.
9. Bismuto E, Irace G. The effect of molecular confinement on the conformational dynamics of the native and partly folded state of apomyoglobin. *FEBS Lett* 2001;509:476–480.
10. Kinjo AR, Takada SJ. Competition between protein folding and aggregation with molecular chaperones in crowded solutions: Insight from mesoscopic simulations. *Biophys J* 2003;85:3521–3531.
11. Ren GP, Lin Z, Tsou CL, Wang CC. Effects of macromolecular crowding on the unfolding and the refolding of D-Glyceraldehyde-3-Phosphosphate dehydrogenase. *J Prot Chem* 2003;22:431–439.
12. Munishkina LA, Cooper EM, Uversky VN, Fink AL. The effect of macromolecular crowding on protein aggregation and amyloid fibril formation. *J Mol Recognit* 2004;17:1–9.
13. Betancourt MR, Thirumalai D. Exploring the kinetic requirements for enhancement of protein folding rates in the GroEL cavity. *J Mol Biol* 1999;287:627–644.
14. Chan HS, Dill KA. A simple model of chaperonin-mediated protein folding. *Proteins* 1996;24:345–351.
15. Zahn R, Perrett S, Fersht AR. Conformational states bound by the molecular chaperones GroEL and SecB: A hidden unfolding (annealing) activity. *J Mol Biol*, 1996;261:43–61.
16. Vaart AVD, Ma JP, Karplus M. 2004. The unfolding action of GroEL on a protein substrate. *Biophys J* 2004;87:562–573.
17. Lundin VF, Stirling PC, Reino JG, Mwenifumbo JC, Obst JM, Valpuesta JM, Leroux MR. Molecular clamp mechanism of substrate binding by hydrophobic coiled-coil residues of the archaeal chaperone prefoldin. *Proc Natl Acad Sci USA* 2004;101:4367–4372.
18. Jewett AI, Baumketner A, Shea JE. Accelerated folding in the weak hydrophobic environment of a chaperonin cavity: creation of an alternate fast folding pathway. *Proc Natl Acad Sci USA* 2004;101:13192–13197.
19. Fink AL. Chaperone-mediated protein folding. *Physiol Rev* 1999;79:425–449.
20. Hartl FU, Hayer-Hartl M. Molecular chaperones in the cytosol: From nascent chain to folded protein. *Science* 2002;295:1852–1858.
21. Creighton TE. Molecular chaperones: unfolding protein folding. *Nature* 1991;352:17–18.
22. Saibil H, Zheng D, Roseman AM, Hunter AS, Watson GMF, Chen

- S, auf der Mauer A, O'Hara BP, Wood SP, Mann NH, Barnett LK, Ellis RJ. ATP includes large quaternary rearrangements in a cage-like chaperonin structure. *Curr Biol* 1993;3:265–273.
23. Thirumalai D, Klimov DK, Lorimer GH. Caging helps proteins fold. *Proc Natl Acad Sci USA* 2003;100:11195–11197.
 24. Minton AP. Implications of macromolecular crowding for protein assembly. *Curr Opin Struct Biol* 2000;10:34–39.
 25. Walter S, Lorimer GH, Schmid FX. A thermodynamic coupling mechanism for GroEL-mediated unfolding. *Proc Natl Acad Sci USA* 1996;93:9425–9430.
 26. Baumketner A, Jewett A, Shea J E. Effects of confinement in chaperonin assisted protein folding: rate enhancement by decreasing the roughness of the folding energy landscape. *J Mol Biol* 2003;332:701–713.
 27. Brinker A, Pfeifer G, Kerner MJ, Naylor DJ, Hartl FU, Hayer-Hartl M. Dual function of protein confinement in chaperonin-assisted protein folding. *Cell* 2001;107:223–233.
 28. Todd MJ, Lorimer GH, Thirumalai D. Chaperonin-facilitated protein folding: optimization of rate and yield by an iterative annealing mechanism. *Proc Natl Acad Sci USA* 1996;93:4030–4035.
 29. Thirumalai D, Lorimer GH. Chaperonin-mediated protein folding. *Annu Rev Biophys Biomol Struct* 2001;30:245–269.
 30. Shtilerman M, Lorimer GH, Englander SW. Chaperonin function: folding by forced unfolding. *Science* 1999;284:822–825.
 31. Eggers DK, Valentine J. Molecular confinement influences protein structure and enhances thermal protein stability. *Prot Sci* 2001;10:250–261.
 32. Bolis D, Politou AS, Kelly G, Pastore A, Temussi PA. Protein stability in nanocages: a novel approach for influencing protein stability by molecular confinement. *J Mol Biol* 2004;336:203–212.
 33. Klimov DK, Newfield D, Thirumalai D. Simulations of β -hairpin folding confined to spherical pores using distributed computing. *Proc Natl Acad Sci USA* 2002;99:8019–8024.
 34. Zhou HX, Dill KA. Stabilization of protein in confined spaces. *Biochemistry* 2001;40:11289–11293.
 35. Takagi F, Koga N, Takada SJ. How protein thermodynamics and folding mechanisms are altered by the chaperonin cage: molecular simulations. *Proc Natl Acad Sci USA* 2003;100:11367–11372.
 36. Stenberg G, Fersht AR. Folding of Barnase in the presence of the molecular chaperone SecB. *J Mol Biol* 1997;274:268–275.
 37. Itzhaki LS, Otzen DE, Fersht AR. Nature and consequence of GroEL-protein interactions. *Biochemistry* 1995;34:14581–14587.
 38. Ma JP, Karplus M. The allosteric mechanism of the chaperonin GroEL: a dynamic analysis. *Proc Natl Acad Sci USA* 1998;95:8502–8507.
 39. Thirumalai D. Theoretical perspectives on in vitro and in vivo protein folding. In: Doniach S, editor. *Statistical mechanics, protein structure, and protein substrate interactions*. New York: Plenum Press; 1994. p 115–134.
 40. Orland H, Thirumalai D. A kinetic model for chaperonin assisted folding of protein. *J Phys I (France)* 1997;7:553–560.
 41. Gorse D. Application of a chaperone-based refolding method to two- and three-dimensional off-lattice protein models. *Biopolymers* 2002;64:146–160.
 42. Friedel M, Sheeler DJ, Shea JE. Effects of confinement and crowding on the thermodynamics and kinetics of folding of a minimalist β -barrel protein. *J Chem Phys* 2003;118:8106–8113.
 43. Gō N. Theoretical studies of protein folding. *Annu Rev Biophys Bioeng* 1983;12:183–210.
 44. Clementi C, Nymeyer H, Onuchic JN. Topological and energetic factors: what determines the structural details of the transition state ensemble and “en-route” intermediates for protein folding? An investigation for small globular proteins. *J Mol Biol* 2000;298:937–953.
 45. Clementi C, Jennings PA, Onuchic JN. Prediction of folding mechanism for circular-permuted proteins. *J Mol Biol* 2001;311:879–890.
 46. Clementi C, Jennings PA, Onuchic JN. How native-state topology affects the folding of dihydrofolate reductase and interleukin-1 β . *Proc Natl Acad Sci USA* 2000;97:5871–5876.
 47. Karanicolas J, Brooks III CL. Improved Gō-like models demonstrate the robustness of protein folding mechanisms towards nonnative interactions. *J Mol Biol* 2003;334:309–325.
 48. Koga N, Takada SJ. Roles of native topology and chain-length scaling in protein folding: a simulation study with a Gō-like model. *J Mol Biol* 2001;313:171–180.
 49. Hoang TX, Cleplak M. Molecular dynamics of folding of secondary structures in Gō-type models of proteins. *J Chem Phys* 2000;112:6851–6862.
 50. Head-Gordon T, Brown S. Minimalist models for protein folding and design. *Curr Opin Struct Biol* 2003;13:160–167.
 51. Zhang J, Qin M, Wang W. Multiple folding mechanisms of protein ubiquitin. *Proteins* 2005;59:565–579.
 52. Chen J, Wang J, Wang W. Transition states for folding of circular-permuted proteins. *Proteins* 2004;57:153–171.
 53. Levy Y, Wolynes PG, Onuchic JN. Protein topology determines binding mechanism. *Proc Natl Acad Sci USA* 2004;101:511–516.
 54. Stoycheva AD, Brooks III CL, Onuchic JN. Gatekeepers in the ribosomal protein s6: thermodynamics, kinetics, and folding pathways revealed by a minimalist protein model. *J Mol Biol* 2004;340:571–585.
 55. Plotkin SS. Speeding protein folding beyond the Gō model: How a little frustration sometimes helps. *Proteins* 2001;45:337–345.
 56. Chol JH, Sato S, Raleigh DP. Thermodynamics and kinetics of nonnative interactions in protein folding: a single point mutant significantly stabilizes the n-terminal domain of L9 by modulating nonnative interactions in the denatured state. *J Mol Biol* 2004;338:827–837.
 57. Paci E, Vendruscolo M, Karplus M. Native and nonnative interactions along protein folding and unfolding pathways. *Proteins* 2002;47:379–392.
 58. Friel CT, Beddard GS, Radford SE. Switching two-state to three-state kinetics in the helical protein Im9 via the optimization of stabilizing nonnative interactions by design. *J Mol Biol* 2004;342:261–273.
 59. Wang J, Wang W. A computational approach to simplifying the protein folding alphabet. *Nat Struct Biol* 1999;6:1033–1038.
 60. Li H, Tang C, Wingreen NS. Nature of driving force for protein folding: a result from analyzing the statistical potential. *Phys Rev Lett* 1997;79:765–768.
 61. Onuchic JN, Nymeyer H, Garcia AE, Chahine J, Socci ND. The energy landscape theory of protein folding: insight into folding mechanisms and scenarios. *Adv Prot Chem* 1999;53:87–152.
 62. Sigler PB, Xu Z, Rye HS, Burston SG, Fenton WA, Horwich AL. Structure and function in GroEL-mediated protein folding. *Annu Rev Biochem* 1998;67:581–608.
 63. Braig K, Otwinowski Z, Hegde R, Boisvert DC, Joachimiak A, Horwich AL, Sigler PB. The crystal structure of the bacterial chaperonin GroEL at 2.8Å. *Nature* 1994;371:578–586.
 64. Xu Z, Horwich AL, Sigler PB. The crystal structure of the asymmetric GroEL-GroES-(ADP)₇ chaperonin complex. *Nature* 1997;388:741–750.
 65. Hunt JF, Weaver AJ, Landry SJ, Gierasch L, Deisenhofer J. The crystal structure of the GroES co-chaperonin at 2.8Å resolution. *Nature* 1996;379:37–49.
 66. Weissman JS, Kashi Y, Fenton WA, Horwich AL. GroEL-mediated folding proceeds by multiple rounds of binding and release of nonnative forms. *Cell* 1994;78:693–702.
 67. Todd MJ, Viitanen PV, Lorimer GH. Dynamics of the chaperonin ATPase cycle: implications for facilitated protein folding. *Science* 1994;256:659–666.
 68. Laminet AA, Ziegelhoffer T, Georgopoulos C, Pluckthun A. The Escherichia coli heat shock proteins GroEL and GroES modulate the folding of β -lactamase precursor. *EMBO J* 1990;9:2315–2319.
 69. Stan G, Thirumalai D, Lorimer GH, Brooks BR. Annealing function of GroEL: structural and bioinformatic analysis. *Biophys Chem* 2003;100:453–467.
 70. Ewalt KL, Hendrick JP, Houry WA, Hartl FU. In vivo observation of polypeptide flux through the bacterial chaperonin system. *Cell* 1997;90:491–500.
 71. Mayhew M, Da Silva ACR, Martin J, Erdjument-Bromage H, Tempst P, Hartl FU. Protein folding in the central cavity of the GroEL-GroES chaperonin complex. *Nature* 1996;379:420–426.
 72. Weissman JS, Rye HS, Fenton WA, Beechem JM, Horwich AL. Characterization of the active intermediate of a GroEL-GroES-mediated protein folding reaction. *Cell* 1996;84:481–490.
 73. Lin Z, Schwarz FP, Eisenstein E. The hydrophobic nature of GroEL-substrate binding. *J Biol Chem* 1995;270:1011–1014.
 74. Klimov DK, Thirumalai D. Cooperativity in protein folding: From lattice models with sidechains to real proteins. *Fold Des* 1998;3:127–139.
 75. Kaya H, Chan HS. Polymer principles of protein calorimetric two-state cooperativity. *Proteins* 2000;40:637–661.

76. Corrales FJ, Fersht AR. The folding of GroEL-bound barnase as a model for chaperonin-mediated protein folding. *Proc Natl Acad Sci USA* 1995;92:5326–5330.
77. Corrales FJ, Fersht AR. Toward a mechanism for GroEL-GroES chaperone activity: an ATPase-gated and -pulsed folding and annealing cage. *Proc Natl Acad Sci USA* 1996;93:4509–4512.
78. Ravindra R, Zhao S, Gies H, Winter R. Protein encapsulation in mesoporous silicate: the effects of confinement on protein stability, hydration, and volumetric properties. *J Am Chem Soc* 2004;126:12224–12225.
79. Ferrenberg AM, Swendsen RH. Optimized monte carlo data analysis. *Phys Rev Lett* 1989;63:1195–1198.
80. Koehl P. Protein structure similarities. *Curr Opin Struct Biol* 2001;11:348–353.
81. Lindberg M, Tangrot J, Oliveberg M. Complete change of the protein folding transition state upon circular permutation. *Nat Struct Biol* 2002;9:818–822.
82. Koradi R, Billeter M, Wüthrich K. MOLMOL: a program for display and analysis of macromolecular structures. *J Mol Graph* 1996;14:51–55.
83. Zahn R, Perrett S, Stenberg G, Fersht AR. Catalysis of amide proton exchange by the molecular chaperones GroEL and SecB. *Science* 1996;271:642–645.
84. Itzhaki L, Otzen D, Fersht AR. The structure of the transition state for folding of chymotrypsin inhibitor 2 analyzed by protein engineering methods: evidence for a nucleation-condensation mechanism for protein folding. *J Mol Biol* 1995;254:260–288.
85. Hansch C, Leo A. Substituent constants for correlation analysis in chemistry and biology. New York: Wiley-Interscience; 1979.
86. Goldberg MS, Zhang J, Sondek S, Matthews CR, Fox RO. Native-like structure of a protein-folding intermediate bound to the chaperonin GroEL. *Proc Natl Acad Sci USA* 1997;94:1080–1085.
87. Peralta D, Hartman DJ, Hoogenraad NJ, Høj PB. Generation of a stable folding intermediate which can be rescued by the chaperonins GroEL and GroES. *FEBS Lett* 1994;339:45–49.
88. Schmidt M, Buchner J, Todd MJ, Lorimer GH, Viitanen PV. On the role of groES in the chaperonin-assisted folding reaction. *J Biol Chem* 1994;269:10304–10311.
89. Fisher MT. Promotion of the in vitro renaturation of dodecameric glutamine synthetase from *Escherichia coli* in the presence of GroEL (chaperonin-60) and ATP. *Biochemistry* 1992;31:3955–3963.
90. Rye SH, Burston SG, Fenton WA, Beechem JM, Xu ZH, Sigler PB, Horwich AL. Distinct actions of cis and trans ATP within the double ring of the chaperonin GroEL. *Nature* 1997;388:792–798.
91. Gray TE, Fersht AR. Refolding of Barnase in the presence of GroEL. *J Mol Biol* 1993;232:1197–1207.
92. Shimizu S, Chan HS. Temperature dependence of hydrophobic interactions: a mean force perspective, effects of water density, and nonadditivity of thermodynamic signatures. *J Chem Phys* 2000;113:4683–4700.
93. Shimizu S, Chan HS. Configuration dependent heat capacity of pairwise hydrophobic interactions. *J Am Chem Soc* 2001;123:2083–2084.
94. Chan HS, Dill KA. Protein folding in the landscape perspective: Chevron plots and nonArrhenius kinetics. *Proteins* 1998;30:2–33.